

國立交通大學

照明與能源光電研究所

碩士論文

Stencil-LPD 色序法

應用於無彩色濾光片之高畫質 120Hz 顯示器



Stencil-LPD Method for High Quality Color Filter-Less

120Hz Field-Sequential-Color Displays.

研究生：張綺文

指導教授：許根玉 教授

黃乙白 教授

中華民國 101 年 7 月

Stencil-LPD 色序法

應用於無彩色濾光片之高畫質 120Hz 顯示器

Stencil-LPD Method for High Quality Color Filter-Less
120Hz Field-Sequential-Color Displays.

研 究 生：張綺文

Student : Chi-Wen Chang

指 導 教 授：許根玉

Advisor : Ken-Yu Hsu

黃乙白

Yi-Pai Huang



國立交通大學
照明與能源光電研究所

碩 士 論 文

A Thesis

Submitted to Institute of Lighting and Energy Photonics

College of Photonics

National Chiao Tung University

in partial Fulfillment of the Requirements

for the Degree of

Master

In

Lighting and Energy Photonics

July, 2012

Tainan, Taiwan, Republic of China

中華民國 101 年 7 月

Stencil-LPD 色序法

應用於無彩色濾光片之高畫質 120Hz 顯示器

碩士研究生：張綺文 指導教授：許根玉教授

黃乙白副教授

國立交通大學光電學院 照明與能源光電研究所

摘 要

色序型液晶顯示器由於不需彩色濾光片，因此有潛力成為次世代節能型綠色顯示器。傳統色序型液晶顯示器以 180Hz 的場率，時序性地顯示紅色、綠色以及藍色色場的畫面，利用人眼在視網膜上的積分而形成一全彩的影像。而考慮到現行主要液晶模態的反應時間，雙色場色序法(120Hz)較能提供足夠的反應時間。因此，雙色場色序法已成為現今發展的主流。

然而，只有兩個場卻要顯示由三原色所組成之全彩影像，缺少了一個自由度，導致畫面嚴重失真。為此，先前的演算法為加上特殊彩色濾光片形成雙色場雙彩色濾光片，如此一來可得到完全不失真的影像，但是卻因加上彩色濾光片而降低了光的穿透率，且多了特殊彩色濾光片的成本。另一種演算法則是將人眼最不敏感的藍色資訊分成兩部份分別與紅色及綠色資訊做結合，這種演算法的優點為不需彩色濾光片，但卻犧牲了影像的藍色資訊。

故此研究提出一新型的雙色場色序法，Stencil-LPD，可根據影像內容選取出最適合的背光訊號，如此一來便可降低因自由度不足而造成的影像失真。此演算法與先前 two-color-field 方法相較之下，有效將影像失真度降低至原先之 53%。另外，由於此演算法提供一較低但卻足夠飽和的顏色做為背光訊號，以降低在色帶拖出時兩個色場的差異，其相對色分離也由原先的 89%改善至 64%。

Stencil-LPD Method for High Quality Color Filter-Less 120Hz Field-Sequential-Color Displays

**Student: Chi-Wen Chang Advisor: Dr. Ken-Yu Hsu
Dr. Yi-Pai Huang**

**Lighting and Energy Photonics Institute
National Chiao Tung University**

Abstract

Since a field-sequential-color LCD (FSC-LCD) does not require color filters, it has potential to be the next-generation eco-display. The conventional FSC-LCD sequentially flashes red, green, and blue field images at 180Hz field rate to form a full color image by the integration on the retina. Considering the currently used LC modes, a two-field method driving at a field rate of 120Hz has been the mainstream to develop.

However, only two fields to display full color images formed by the three primaries, it is lack of a degree of freedom resulting image distortion. Thus, in the previous solutions, a specific color filter was applied, known as the 2F2CF method proposed by Phillips. By doing so, it can reproduce exactly the same image with the original one but still needs color filters. The other method, two-color-field proposed by NCTU, is to divide the blue information, which is the least sensitive color to human eyes, into two parts and to combine them with red and green information individually. This method does not require color filters but cause color distortion.

In this thesis, a novel two-field display method, Stencil-LPD, was proposed without color filters. The Stencil-LPD method can provide proper backlight colors according to the image content that can decrease the color difference caused by the lack of degree of freedom. Compared to the two-color-field method, the proposed method reduced the color distortion by 53%. Besides, Stencil-LPD method provided less but sufficient saturation colors as backlight signals, the chrominance difference was lowered that diminishes the relative CBU value to 64% while it is 89% in the two-color-field method.

誌 謝

首先誠摯的感謝謝漢萍老師與黃乙白老師對於研究、態度以及英語能力上的指導與培養，並且提供了豐富的資源以及完善的研究環境，使我得以在碩士生涯中能夠心無旁騖的提升自己的專業以及英文能力，順利完成此論文。另外，更要感謝指導教授許根玉老師在各方面的幫助，也感謝每位口試委員所提供的寶貴意見，使得本論文更加完善。

另外，此篇論文能夠順利完成要特別感謝林芳正學長的指導。兩年來學長一路引導、協助並且鼓勵我，學長嚴謹的研究態度以及做事方式，無論在學術上或是生活上都讓我學到很多，也成長了很多。也要感謝同組的學長姐們，政育、宜如、怡伶、瑋玲、期竹、世勛、毅翰、昌毅，在這兩年來的指導與協助，當我有問題時不吝惜的給我幫助及建議。

兩年的研究生活，感謝有小皮、致維哥、大頭、奕智、博全、精益、國振、志明、台翔等學長姐們提供各方面的指導與分享，也謝謝小馬、思頤、小頭、小董、馬爺、博六、博詮、立偉、小發特、濟宇以及子寬，讓我的生活更加精彩。感謝拉拉、博凱、白諭陪我度過了許多難熬的時刻，另外還有上翰、秉彥、囧務、柏皓、博鈞、岡儒陪我一起留下了美好且精彩的回憶。你們在課業、研究與生活上的討論與分享讓我又有了不同的體驗，和你們的相處十分的開心。也謝謝助理姐姐們，雅惠、穎佳、茉莉、蓮芳以及學弟們在各方面事情的處理上盡了很多心力，讓我們毫無後顧之憂也讓實驗室充滿了歡樂的氣氛。

最重要的，我要感謝我最親愛的家人，謝謝爸媽和哥哥的支持與體諒，還有求學路程上的鼓勵，從不讓我感受到壓力，讓我可以毫無顧慮的專注在學習上。也要感謝我的姐妹們，腰、佻、珊及初，謝謝你們在各方面給我的幫助，並且忍受我的壞脾氣，在我灰心喪志的時候幫我打氣，陪著我一路走到現在。除此之外，感謝交大羽球隊，尤其是阿蠢、玉婷、小高、阿煩、大叔、筱涵、林琳和小花，以及教練廖威彰老師，這兩年來對我特別的包容和鼓勵，更提供我一個抒解情緒的好地方。在此，我要將這份喜悅分享給所有我愛的以及愛我的人。



Content

| | |
|---|-----------|
| 摘 要 | i |
| Abstract | ii |
| 誌 謝 | iii |
| Chapter 1 | 1 |
| 1.1 Field-Sequential-Color LCDs (FSC-LCDs) | 1 |
| 1.2 Color Breakup Phenomenon (CBU) | 5 |
| 1.3 Motivation and objective | 6 |
| 1.4 Organization | 7 |
| Chapter 2 | 8 |
| 2.1 Human Visual System | 8 |
| 2.2 Color Breakup Mechanism | 10 |
| 2.2.1 Dynamic Color Breakup | 10 |
| 2.2.2 Static Color Breakup | 11 |
| 2.3 Color space transformation and evaluation index of color difference | 12 |
| 2.3.1 Color space transformation | 12 |
| 2.3.2 Color difference of CIEDE2000 | 18 |
| 2.4 Prior Color Breakup Suppression Methods | 19 |
| 2.4.1 Motion compensation | 19 |
| 2.4.2 Mono-color fields | 21 |
| 2.4.3 Multi-color fields | 22 |
| 2.5 Summary | 28 |
| Chapter 3 | 30 |
| 3.1 Concept | 30 |
| 3.2 Algorithm | 32 |
| 3.2.1 Backlight determination | 32 |

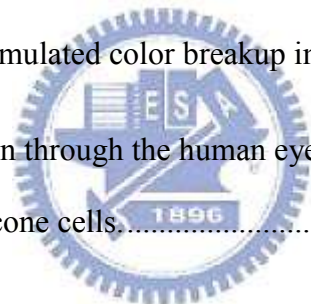


| | |
|--|-----------|
| 3.2.2 LC calculation | 34 |
| 3.3 Simulation results | 37 |
| 3.4 Discussion..... | 40 |
| 3.5 Summary..... | 41 |
| Chapter 4..... | 42 |
| 4.1 Backlight Division Optimization..... | 42 |
| 4.2 Results | 43 |
| 4.2.1 Color Difference Maps | 43 |
| 4.2.2 Demonstration Results..... | 45 |
| 4.3 Comparison..... | 47 |
| 4.4 Summary..... | 48 |
| Chapter 5..... | 49 |
| 5.1 Conclusion..... | 49 |
| 5.2 Future Works | 49 |
| References | 51 |



Figure Captions

| | |
|--|----|
| Fig. 1. The structure of the TFT LCD. | 2 |
| Fig. 2. The structure of the FSC-LCD. | 3 |
| Fig. 3. Temporal color mixing to form a full-color image..... | 3 |
| Fig. 4. The timing chart in a frame time of FSC-LCD. | 4 |
| Fig. 5. Public Information Displays (PIDs) applications on (a) scoreboards and (b) vending machines. | 5 |
| Fig. 6. (a) Target image, and (b) simulated color breakup image with 10 pixels shifted. | 6 |
| Fig. 7. A drawing of a cross-section through the human eye with a schematic enlargement of the retina including rod cells and cone cells. | 9 |
| Fig. 8. A schematic drawing of rods and cones cell. | 9 |
| Fig. 9. Response of the three human cone types to the light of different wavelengths. | 10 |
| Fig. 10. The mechanism of perceiving dynamic color breakup. | 11 |
| Fig. 11. The perception mechanism of static color breakup. | 12 |
| Fig. 12. Experimental setup of color-matching experiments..... | 13 |
| Fig. 13. (a) Tristimulus values for different wavelengths, and (b) CIE 1931 (R, G, B) chromaticity diagram. | 13 |
| Fig. 14. CIE 1931 (X, Y, Z) chromaticity diagram. | 15 |
| Fig. 15. MacAdam ellipses in the CIE 1931 (X, Y, Z) chromaticity diagram. | 16 |



| | |
|---|----|
| Fig. 16. CIELAB color space. | 17 |
| Fig. 17. CIE1976 $u'v'$ chromaticity diagram..... | 18 |
| Fig. 18. The mechanism of motion compensation; color breakup was suppressed effectively. | 20 |
| Fig. 19. The mechanism of motion compensation; object and observer's eye tracing path are in the opposite position..... | 21 |
| Fig. 20. Simulation color breakup image of (a) 180Hz RGB, and (b) 360Hz RGBRGB. | 22 |
| Fig. 21. Simulation color breakup image of (a) 180Hz RGB, and (b) 300Hz RGBCY. | 22 |
| Fig. 22. The concept of Stencil-FSC methods: (a) 240Hz Stencil-FSC (b) 180Hz Stencil-FSC. | 23 |
| Fig. 23. Color breakup of image <i>Girl</i> by different FSC methods: (a) RGB-driving, (b) the 240Hz Stencil-FSC method..... | 24 |
| Fig. 24. The concept of LPD method. (a)The target image, <i>lily</i> . (b)The three fields of RGB driving (left) and the LPD method (right). (c)Color breakup simulation with 15 pixels shifted for each field using RGB driving (left) and the LPD method (right)..... | 25 |
| Fig. 25. The triangles represent color saturation of sRGB and LPD backlight primary-colors in the CIE1976 $u'v'$ uniform color space. | 26 |
| Fig. 26. A 2F2CF type with yellow-cyan (Y-C) backlights and green-magenta (G-M) color filters. (a)Spectrum-level illustration for the color synthesis procedure. (b)The configuration of type-I 2F2CF LCD. | 27 |
| Fig. 27. Another 2F2CF type with green-magenta (G-M) backlights and yellow-cyan (Y-C) color filters. (a)Spectrum-level illustration for the color synthesis procedure. (b)The | |



| | |
|--|----|
| configuration of type-II 2F2CF LCD. | 27 |
| Fig. 28. Two driving schemes, a 180Hz RGB driving type and the two-color-field method. By field decomposition of color fields to form full-color image. | 28 |
| Fig. 29. (a) A test image and one of backlight segments with its (b) pixel chromaticity distribution (blue circles) and the backlight chromaticity of two fields (red dots) in the CIE1976 $u'v'$ color space. (c) The reproduced distorted image using the two-color-field FSC method [11]. | 28 |
| Fig. 30. The concept of proposed Stencil-LPD method with (a) pixel chromaticity distribution in one of backlight segments in (b) the test image. According to the color distribution tendency (blue dots), we choose the backlight signals (red dots 1 and 2) for two fields in each segment. | 31 |
| Fig. 31. (a) A test image and one of backlight segments with its (b) pixel chromaticity distribution (blue circles) and the backlight chromaticity of two fields (red dots) in the CIE1976 $u'v'$ color space. (c) The reproduced distorted image using the two-color-field FSC method. | 31 |
| Fig. 32. Flow chart of Stencil-LPD method. | 32 |
| Fig. 33(a) The most represented color of each segment in the first field (up) with compensated LC signals (middle) causes annoying lines. | 34 |
| Fig. 34. The approximation method. | 36 |
| Fig. 35. The driving scheme of Stencil-LPD method. | 37 |
| Fig. 36. Nine test images varying in color saturation and image complexity: Lily, Finger, Polar bear*, Red leaf, Hats, Plane, Teapot#, Sashimi, and Basketball. | 38 |


| | |
|---|----|
| Fig. 37. (a) The PDR ($\Delta E_{00} > 3$) values of nine test images in the two methods and (b) the relative CBU..... | 39 |
| Fig. 38. Hats: (a) The reproduced images and (b) the color difference images by the 120Hz Stencil-LPD (up) and two-color-field FSC methods (down). | 39 |
| Fig. 39. Red leaf: (a) The reproduced images and (b) the color difference images by the 120Hz Stencil-LPD (up) and two-color-field FSC methods (down). | 40 |
| Fig. 40. (a)The distortion happens when there is too many color content in one segment. (b) The chromaticity distribution (blue dots) and the absent information that could not be displayed (in the green circle). | 41 |
| Fig. 41. Ten test images with different image content..... | 43 |
| Fig. 42. The simulation results with indices (a) PDR($\Delta E_{00}>3$) and (b) power..... | 43 |
| Fig. 43. Three test images: (a) Teapot, (b) Girl, and (c) Sunflower..... | 44 |
| Fig. 44. The reproduction results of the three test images..... | 45 |
| Fig. 45. The reproduced images with (a) 2-color-field method and (b) Stencil-LPD method . | 46 |
| Fig. 46. The CBU images by shaking the camera horizontally to simulate eye movement with (a) 2-color-field method and (b) Stencil-LPD method. | 47 |

Chapter 1

Introduction

Liquid crystal display (LCD) is the mainstream of modern display technology. However, the low optical throughput is the main problem around the corner since the concern for energy raises rapidly around the world. Therefore, a field-sequential-color LCD (FSC LCD) without color filter is developed to lower the power consumption. On the other hand, the color breakup (CBU) phenomenon has become a main issue in FSC-LCDs. In this chapter, FSC-LCDs and the color breakup issue will be elaborated, with the motivation and objective of this thesis. The last but not least section is the organization of this thesis.

1.1 Field-Sequential-Color LCDs (FSC-LCDs)



The LCDs have replaced the cathode ray tube (CRT) as commercial display products due to its advantages in weight, volume, and not radiation emitting. However, an LCD is not self-emissive, so it requires a backlight module as the light sources. Backlight module and LC layer are two main components while constructing an LCD. The structure of a TFT-LCD is illustrated in Fig. 1. A full-on white light source is lightened by the backlight module, uniformed by passing through a set of optical films and directed to transmit into the LC layer. The TFT and color filters also reduce light transmittance since the total optical throughput is only about 7% of the total input. Especially, two third of light intensity from the backlight module would be absorbed by color filters.

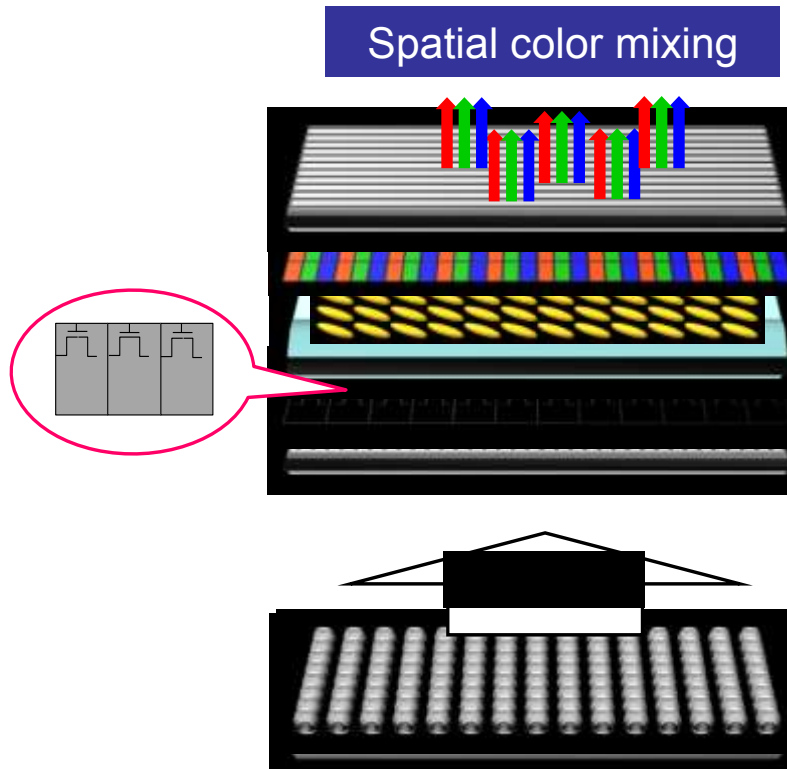


Fig. 1. The structure of the TFT LCD.

The FSC-LCD [1], which is shown in Fig. 2, is a less power consuming display. Without color filters, it increases three times of light transmittance. The FSC-LCD sequentially flashes red, green, and blue field images with RGB LEDs to form a full color image, as shown in Fig. 3 [2]-[6]. Based on the temporal color mixing phenomena, human visual system will combine these images as a full color image. Without color filters, the FSC-LCDs are better than conventional LCDs with lots of advantages such as lower power consumption, higher transmittance, higher possible image resolution, and lower material cost. With these advantages, an FSC-LCD is no doubt a popular next-generation Eco-display.

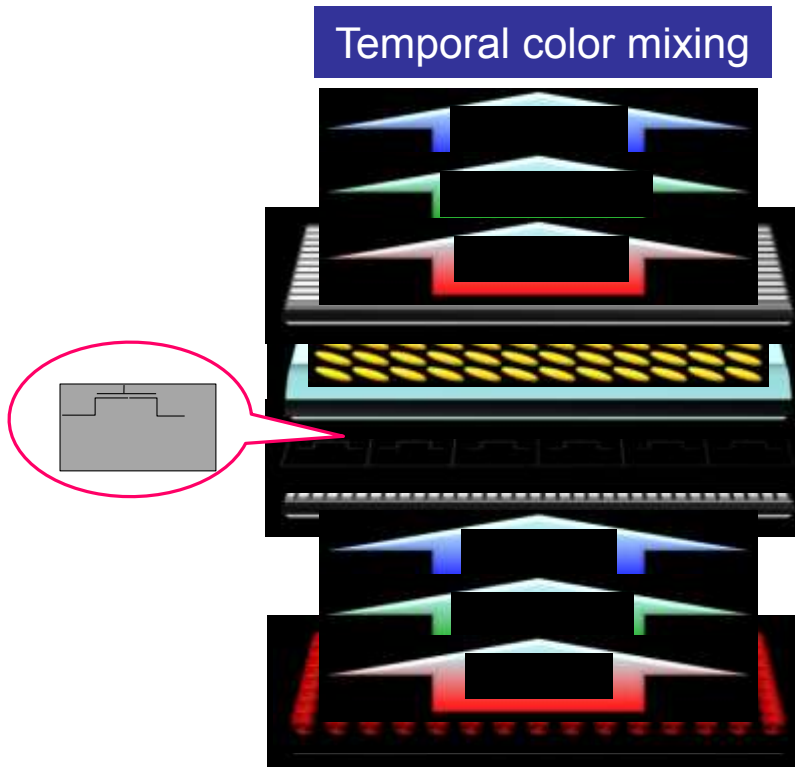


Fig. 2. The structure of the FSC-LCD.

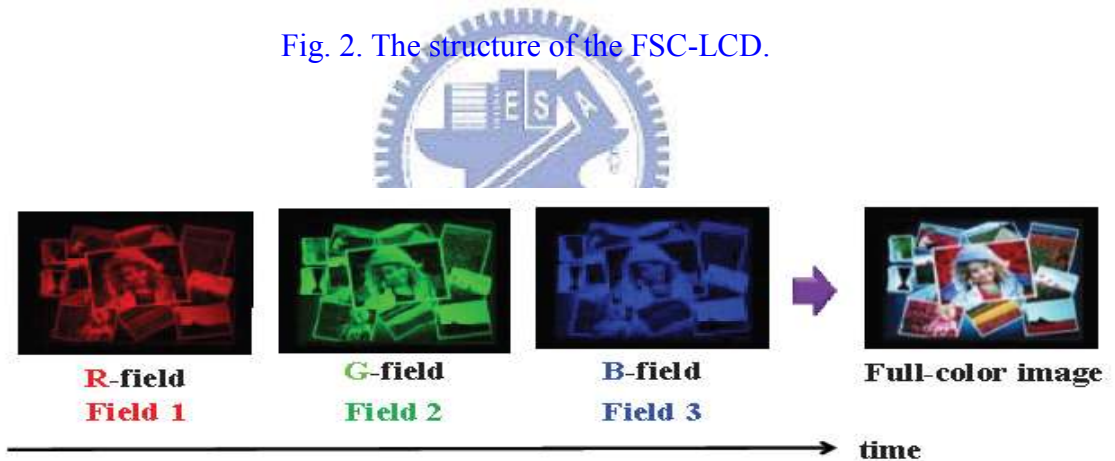


Fig. 3. Temporal color mixing to form a full-color image.

Three main parts are necessary when it comes to driving scheme of FSC-LCDs: the TFT addressing, the LC response, and the backlight flashing. The timing chart is illustrated in Fig. 4; each frame is divided into three fields. The frame rate is 60 Hz as the conventional LCD, avoiding observers from feeling flicker. Thus, the field rate is 180Hz for an RGB driving method, three times higher than the frame rate. In each field, the panel has to complete the steps such as loading data for the whole panel, orientating LC to the right directing angle, and

flashing backlight. After all these steps, the inherent temporal color mixing mechanism in human visual system will generate a full color image.

Besides, public information displays (PIDs), as shown in Fig. 5, are now more and more popular that LEDs (a) and large size LCDs (b) are often applied to. The characteristics of LEDs are high luminance, high color saturation, but low spatial resolution. In contrast, large size LCDs have high resolution but low transmittance and color saturation. Since all PID applications require large size and high luminance, conventional LCDs reduce color saturation to earn higher luminance than usual; while the resolution can be enhanced by increasing the number of LEDs. However, reaching these demands would enlarge the cost. So FSC-LCDs here are more promising to be utilized to achieve higher resolution than LEDs and higher luminance than conventional LCDs.

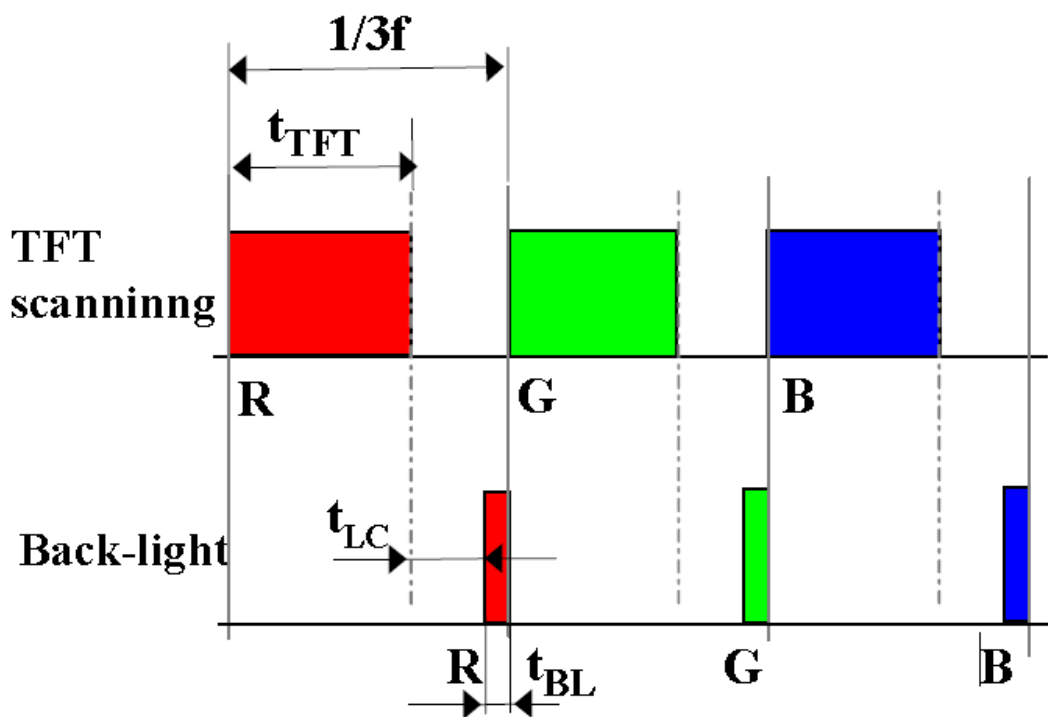


Fig. 4. The timing chart in a frame time of FSC-LCD.



(a) (b)

Fig. 5. Public Information Displays (PIDs) applications on (a) scoreboards and (b) vending machines.

1.2 Color Breakup (CBU) Phenomenon

Without using color filters, field-sequential-color LCDs can perform three times higher optical throughput than conventional LCDs. Nevertheless, due to the way FSC-LCD displaying a colorful image is to sequentially display fields, a serious issue, color breakup (CBU), might come up with the relative speed between the displayed image and the viewer's eyes [7]. CBU looks as a rainbow blur on the object fringe in the image as shown in Fig. 6. The color breakup phenomenon happens when there is relative motion, the separated colors on image edges can be perceived by human eye after visual integration. The CBU phenomenon would degrade image quality and cause discomfortable to human eyes. The mechanism and some prior resolutions of CBU will be further discussed in chapter 2.

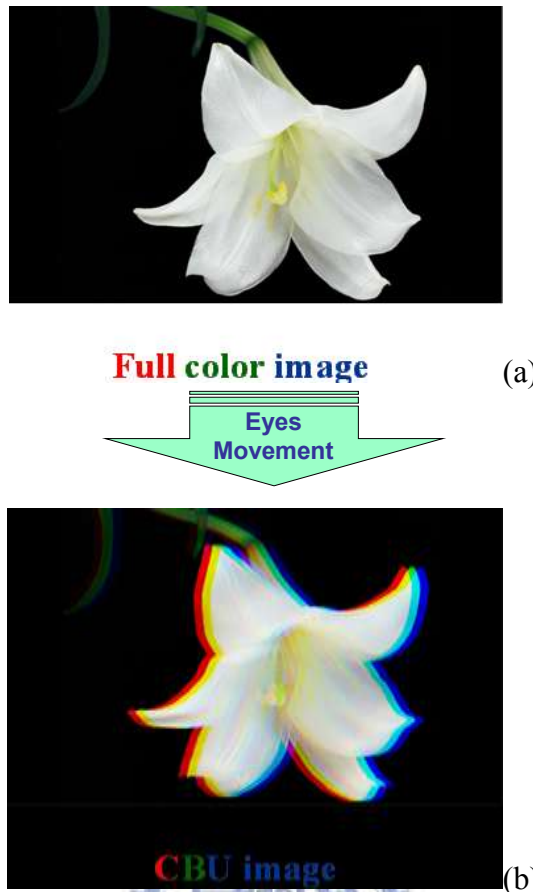


Fig. 6. (a) Target image, and (b) simulated color breakup image with 10 pixels shifted.

1.3 Motivation and objective

Though FSC-LCD has three times higher optical throughput than conventional LCDs, it also has to drive at least three times faster in each pixel. Taking a 60Hz frame rate of RGB FSC method as an example, the field rate is 180Hz, which is only 5.56ms for each field. The length of TFT scanning is more than 3.3ms, and the backlight flashing length of each field is about 1.22ms. Therefore, the LC response time is limited to be shorter than 1ms. Several methods are brought out recent years to save as much time for LC response as possible, such as over-drive [8]-[9], and multi-division backlight [10]. The response time of the commercial LC modes are all longer than 5ms. Even the specific LC mode, nor can optically compensated bend (OCB) mode reach the response time. Thus, a two-color-field driving scheme [11], which allows longer time for LC response in FSC-LCDs and a two-field with two color filters

method (2F2CF) [12][13] were both proposed. However, the two-color-field method needs a large number of backlight divisions to maintain the image fidelity while the 2F2CF method lowers the light transmittance through the special color filters. The detail of these two driving scheme will be further elaborated in chapter 2. Hence, the objective of this thesis is to develop a 120Hz color-filter-less FSC LCD with high image quality, and less number of backlight divisions.

1.4 Organization

This thesis is organized as follows: In **Chapter 2**, the mechanism of causing CBU, some prior arts to solve CBU with multi-color-field, the two-field driving schemes, the color space transforming, the evaluation index for color difference and CBU suppression will be discussed. In **Chapter 3**, the proposed method, 120Hz Stencil-LPD method that can maintain the image fidelity without color filters will be detailed. The concept and algorithm of the proposed method will be illustrated. The simulation results with discussion will be presented at the same time. In **Chapter 4**, the optimization and the final results will be shown. Last but not least, the conclusion and future work will be given in **Chapter 5**.

Chapter 2

Principles

Color filter-less FSC-LCDs have the advantages of higher optical throughput, lower material cost, wider color gamut, and a possibility of three times higher resolution. However, color breakup phenomenon caused by the relative velocity between human eye and screen object degrades the image clarity and discomforts in human eye. Therefore, researches of various color breakup mechanisms and their suppression methods will be discussed in this chapter. In this thesis, color breakup phenomenon is quantified by the evaluation index of modified CIE DE2000.

2.1 Human Visual System



Color breakup phenomenon correlates to the mechanism of human eye. Fig. 7 shows the cross-section of a human eyeball and a schematic enlargement picture of the retina [14]. The reflected light from objects is transmitted and refracted by the lens and eventually projected onto the retina. Retina is a nerve tissue in the eye that is responsible for sensation of light. It converts the optical signals of the visualized object to electrical impulses, which are then sent to the brain via the optical nerve. There are two types of photo-receptors in the human eye; the rods and cones. The rod cells are more abundant than cone cells in the retina, as shown in Fig. 8 [15]. Rod cells are sensitive to low levels of illumination (scotopic vision); the responses of which are slower and are not involved in color vision. On the contrary, cone cells are sensitive to high levels of illumination (photopic vision) with faster responses and produces color vision. Moreover, cone cells are further divided into of S-cones, M-cones, and L-cones according to their responding wavelengths, which are short-wavelength, middle-wavelength,

and long-wavelength respectively as shown in Fig. 9 [16].

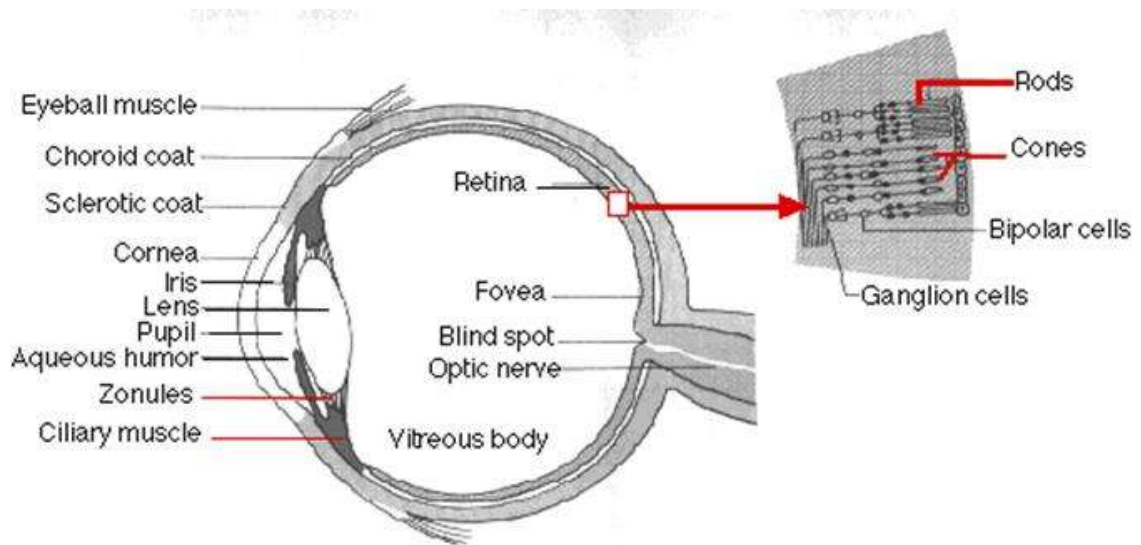


Fig. 7. A drawing of a cross-section through the human eye with a schematic enlargement of the retina including rod cells and cone cells.

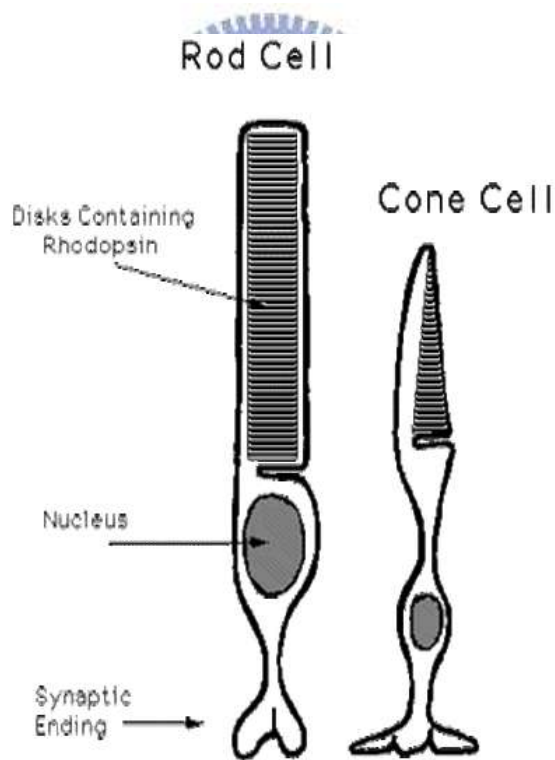


Fig. 8. A schematic drawing of rods and cones cell.

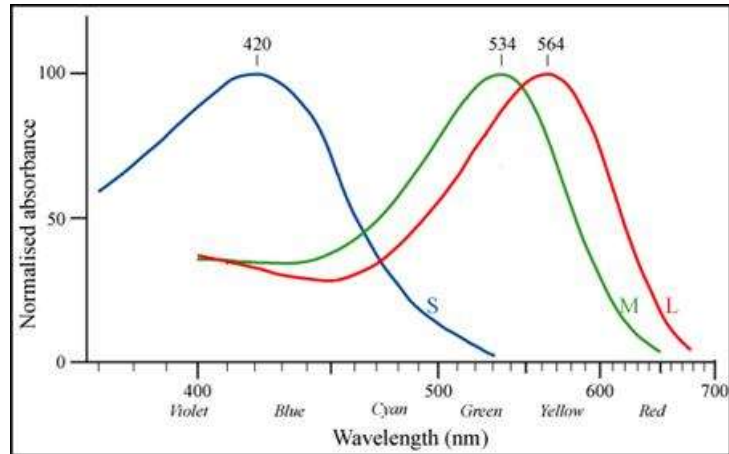


Fig. 9. Response of the three human cone types to the light of different wavelengths.

2.2 Color Breakup Mechanism

Color breakup (CBU) phenomenon occurs when human eye and the displayed object are moving under different speeds. This phenomenon results in not only eyes discomfort but also degrades image quality. Hence, understanding the mechanism of color breakup is necessary in order to come up with ways to inhibit the annoying phenomenon. As mentioned before, color breakup is dependent on the types of eyes movement, saccade or smooth pursuit. Therefore, considering this aspect, color breakup phenomenon can be classified into two types: dynamic color breakup and static color breakup, according to the moving feature of images and eyes movement.

2.2.1 Dynamic Color Breakup

Dynamic color breakup phenomenon mostly occurs on the fringes of moving objects on FSC-LCDs. Fig. 10 shows the perception mechanism of dynamic color breakup [17]. The horizontal axis represents the position in a FSC-LCD while the vertical axis shows time progressing. The colors comprising the white color, which are red, green, and blue, are displayed temporally in one field time. Through eye integration, the three primary-colors are projected and separated onto the retina and results in a rainbow-like color bar on the edges of

the white image, which is then perceived by human eyes. Through eye integration, the three primary-colors are projected onto the retina and a rainbow-like color bar occurring in the edge of white image is perceived by human eye.

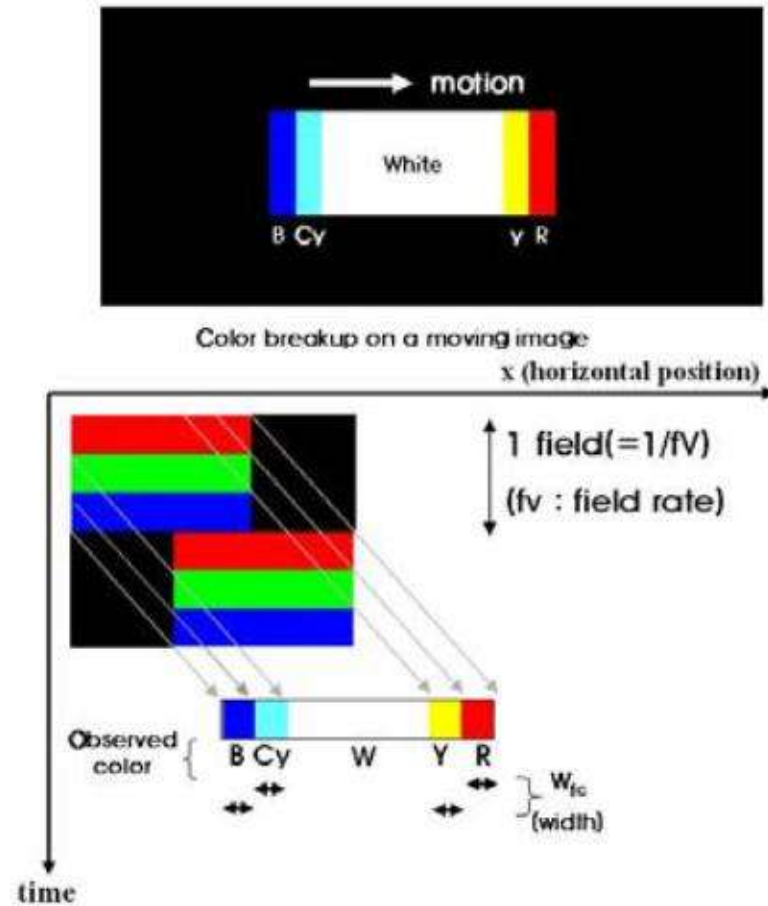


Fig. 10. The mechanism of perceiving dynamic color breakup.

2.2.2 Static Color Breakup

Static color breakup occurs when human eyes glance at a still image. Fig. 11 shows the mechanism of perceiving static color breakup [17]. The fixed white image which consists of the three primary-colors, R, G, and B, is displayed in a FSC-LCD. When human eyes glance at the image to obtain detail features, the R, G, and B sub-field image are projected onto the retina separately. Static color breakup is perceived at the edge of stationary image in this way. Therefore, it is static CBU that makes most people feel uncomfortable because it is more frequently observed than dynamic CBU.

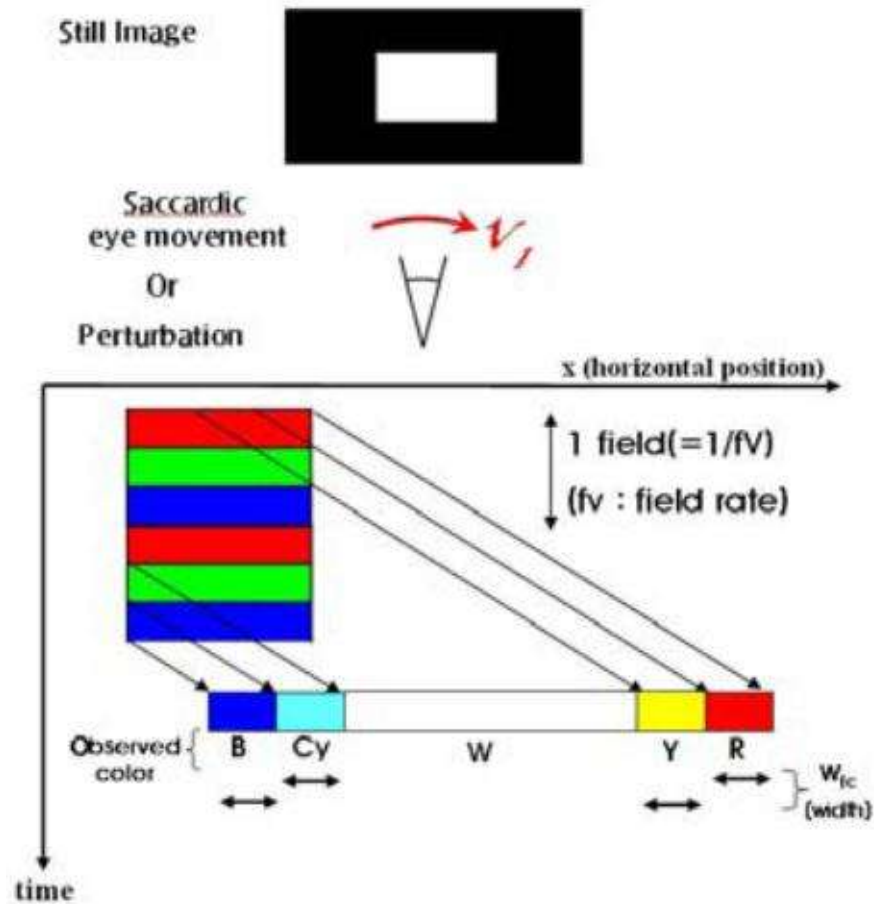


Fig. 11. The perception mechanism of static color breakup.

2.3 Color space transformation and evaluation index of color difference

2.3.1 Color space transformation

Considering the concept of trichromatic color space, every color is mixed by the three primary colors: red, green and blue. Fig. 12 shows the setup of the color-matching experiments [17]. An arbitrary light of the test colors illuminates the lower half of the white screen and produces a visual stimulus to the human eye through the black shadow. Meanwhile, the upper half of the white screen is illuminated by a light source that consists of the three primary colors. The intensities of the red, green and blue light sources are adjusted respectively in order to match the color projected on the lower screen. We see that it is possible to find a set of R, G and B that matches any specific color. In 1931, the CIE used the

three primary colors with wavelengths of 700nm, 546.1nm and 435.8nm to match all visible monochromatic lights as shown in Fig. 13 (a), and the CIE 1931(R, G, B) chromaticity diagram can be obtained as shown in Fig. 13 (b).

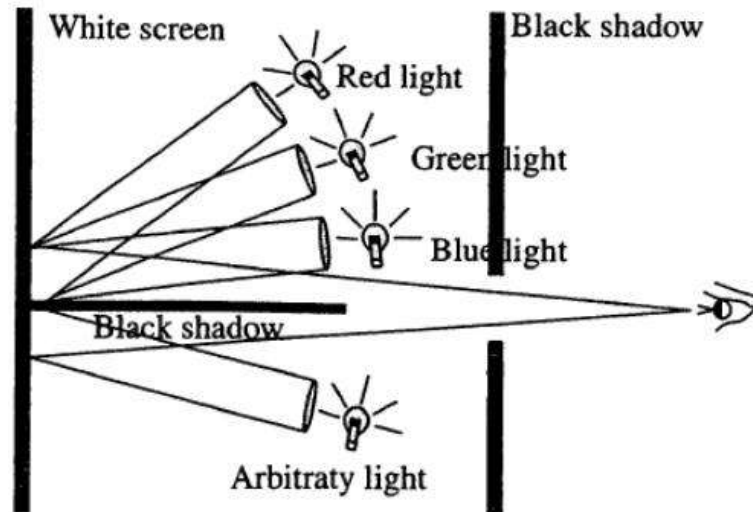


Fig. 12. Experimental setup of color-matching experiments.

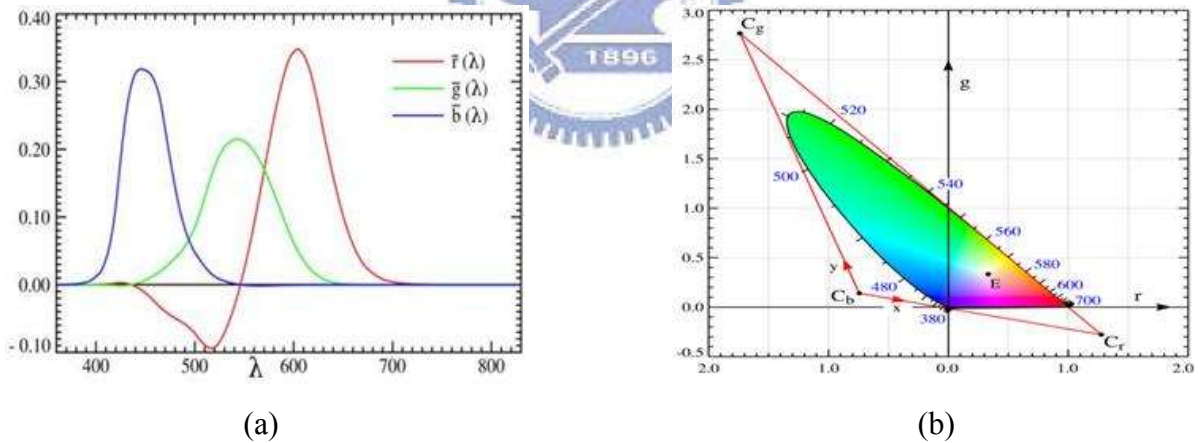


Fig. 13. (a) Tristimulus values for different wavelengths, and (b) CIE 1931 (R, G, B) chromaticity diagram.

Since different color stimuli can be obtained by linear summation, the spectrum of multi-wavelength can be viewed as the color mixing of each monochromatic component. Therefore, any color in the horseshoe-shaped region is blended by monochromatic light between 380 and 780 nm. In the color-matching experiments shown in Fig. 12, some desired

colors cannot be acquired no matter how the (R, G, B) intensities are adjusted. To resolve this issue, we can move one of the primary sources from the upper screen to the lower screen on top of the desired color. As Fig. 13 (b) shows, the negative r values are sometimes not suitable for describing particular colors [19]. To solve this problem, the CIE1931 (X, Y, Z) system was proposed with

$$z = \frac{0.00000r+0.01000g+0.99000b}{0.66697r+1.13240g+1.20063b}$$

Eq. 1, as

shown in Fig. 14. CIE 1931 (X, Y, Z) chromaticity diagram. By using this method, all colors can now be described with positive values. One important feature of the CIE1931 (X, Y, Z) system is that the Y value was set as luminance of the stimulus in terms of lm sr^{-1} or cdm^{-2} . To get the CIE 1931 (X, Y, Z) values from a spectrum, each wavelength is summed linearly as shown in

$$y = \frac{Y}{X+Y+Z}$$



Eq. 2.

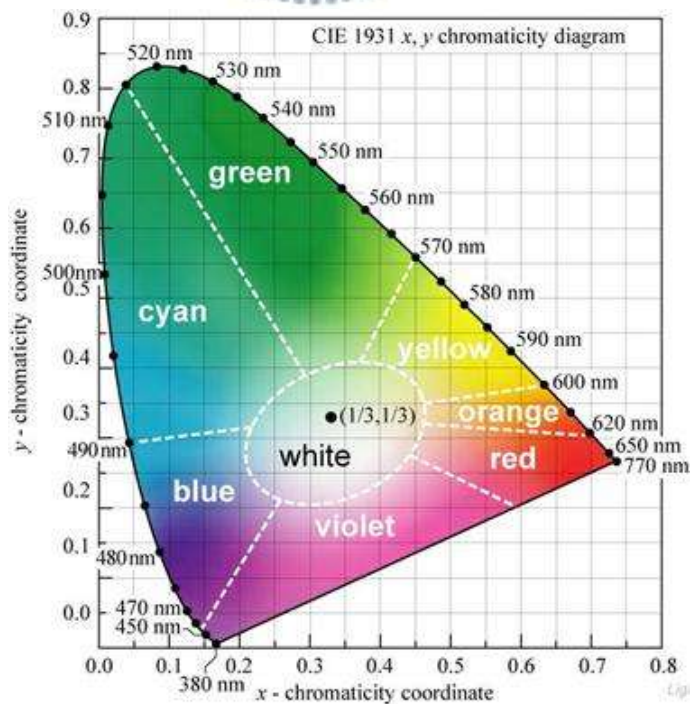


Fig. 14. CIE 1931 (X, Y, Z) chromaticity diagram.

$$x = \frac{0.49000r+0.31000g+0.20000b}{0.66697r+1.13240g+1.20063b}$$

$$y = \frac{0.17697r+0.81240g+0.01063b}{0.66697r+1.13240g+1.20063b}$$

$$z = \frac{0.00000r+0.01000g+0.99000b}{0.66697r+1.13240g+1.20063b}$$

Eq. 1

$$X = k \int_{\lambda} P(\lambda) \bar{x}(\lambda) d(\lambda)$$

$$Y = k \int_{\lambda} P(\lambda) \bar{y}(\lambda) d(\lambda)$$

$$Z = k \int_{\lambda} P(\lambda) \bar{z}(\lambda) d(\lambda)$$

$$x = \frac{X}{X+Y+Z}$$

$$y = \frac{Y}{X+Y+Z}$$



Eq. 2

where $k=683 \text{ lm } W^{-1}$, which represents the transformation from radiometry units (W) to photometry units (lm), and $P(\lambda)$ is the spectral distribution of the stimulus in terms of $W \text{ sr}^{-1} \text{ m}^{-2}$.

Although the CIE 1931 (X, Y, Z) color system can precisely define a color, there is a problem when dealing with color difference and its tolerance [20][21]. Fig. 15 shows the well-known MacAdam ellipses in the CIE 1931 (X, Y, Z) chromaticity diagram [22]. Human eye would not distinguish color difference within the ellipses in this figure. To better illustrate the color difference between two stimuli, a uniform color system is necessary. In 1976, CIE provided the CIELAB and CIELUV color systems as uniform color spaces, which are utilized in industrial applications.

$$\Delta E^*_{ab} = \sqrt{(\Delta L^*)^2 + (\Delta a^*)^2 + (\Delta b^*)^2} \quad \text{Eq.}$$

3 derives the coordinate transform from the CIE 1931 (X, Y, Z) to the 1976 (L*, a*, b*) color system. In the equation, X_n, Y_n, and Z_n are the three tri-stimulus values of reference white. L* represents lightness, a* approximate redness-greenness, and b* approximate yellowness-blueness. Therefore, the color difference is evenly given by the formula of ΔE*_{ab}. The CIELAB provided a uniform chromaticity diagram, as shown in Fig. 16, which makes most of color difference formulas were established based on the CIELAB color space.

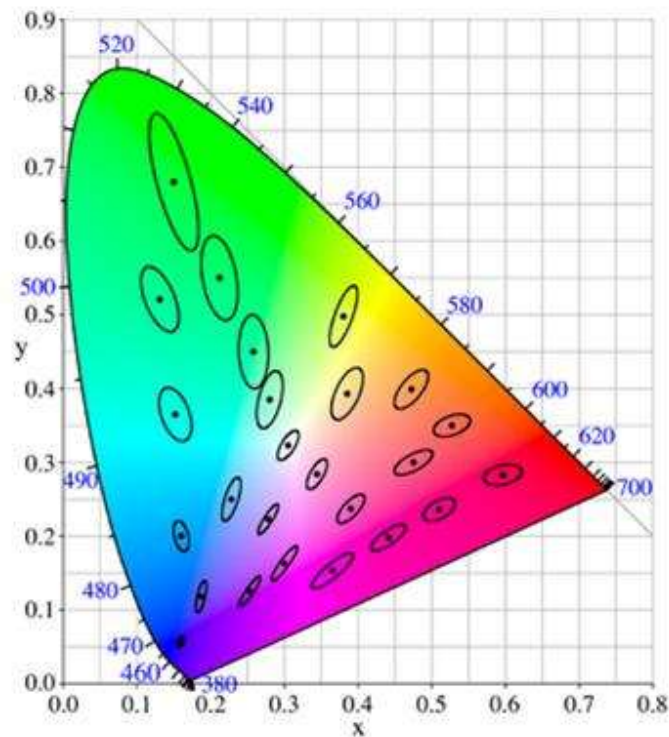


Fig. 15. MacAdam ellipses in the CIE 1931 (X, Y, Z) chromaticity diagram.

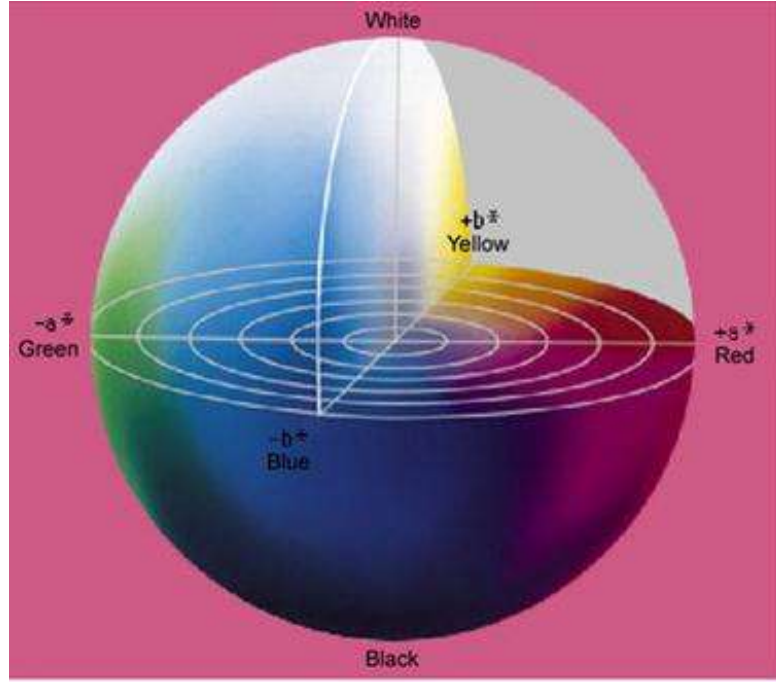


Fig. 16. CIELAB color space.

$$L^* = \begin{cases} 116 \left(\frac{Y}{Y_n} \right)^{\frac{1}{3}} - 16; & \text{for } \frac{Y}{Y_n} > 0.008856 \\ 903.3 \frac{Y}{Y_n}; & \text{for } \frac{Y}{Y_n} \leq 0.008856 \end{cases}$$

$$a^* = 500 \left[f \left(\frac{x}{x_n} \right) - f \left(\frac{y}{y_n} \right) \right];$$

$$b^* = 200 \left[f \left(\frac{y}{y_n} \right) - f \left(\frac{z}{z_n} \right) \right];$$

$$\text{Where } f \left(\frac{y}{y_n} \right) = \begin{cases} \frac{y}{y_n}^{1/3} & \text{for } \frac{y}{y_n} > 0.008856 \\ \frac{1}{3} \left(\frac{29}{6} \right)^2 \frac{y}{y_n} + \frac{16}{116} & \text{for } \frac{y}{y_n} \leq 0.008856 \end{cases}$$

$$\Delta E^*_{ab} = \sqrt{(\Delta L^*)^2 + (\Delta a^*)^2 + (\Delta b^*)^2} \quad \text{Eq. 3}$$

The CIE1976 (L, U, V) color space was adopted as the CIE 1931 (X, Y, Z) color space with perceptual uniformity. It is extensively used for applications such as computer graphics which deal with colored lights.

$$v' = \frac{9Y}{X+15Y+3Z}; \quad \text{Eq. 4}$$

derives the coordinate transform from the CIE 1931 (X, Y, Z) to the 1976 (L, u', v') color

system. This color space is employed to determine backlight signals in this thesis due to its uniform characteristic (Fig. 17).

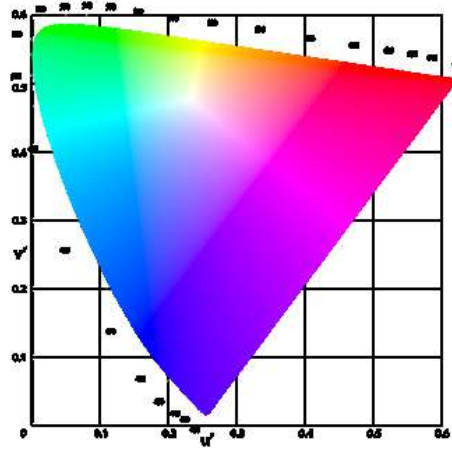


Fig. 17. CIE1976 u'v' chromaticity diagram.

$$u' = \frac{4X}{X+15Y+3Z};$$

$$v' = \frac{9Y}{X+15Y+3Z};$$



Eq. 4

2.3.2 Color difference of CIEDE2000

Based on the color difference of 1976 CIELAB, CIE proposed the CIEDE2000 to modified the formula to describe all color difference ranges [23]-[26]. To revise the issue of color uniformity, the formula, as shown in

$$\Delta E_{00} = \sqrt{\left(\frac{\Delta L^*}{K_L S_L}\right)^2 + \left(\frac{\Delta C_{ab}^*}{K_C S_C}\right)^2 + \left(\frac{\Delta H_{ab}^*}{K_H S_H}\right)^2 + R_T \left(\frac{\Delta C_{ab}^*}{K_C S_C}\right) \left(\frac{\Delta H_{ab}^*}{K_H S_H}\right)} \quad \text{Eq. 5,}$$

considers the weighting function of lightness (S_L), chroma (S_C), and hue (S_H), which are

shown in $S_L = 1, S_C = 1 + 0.045C_{ab}^*, \text{ and } S_H = 1 + 0.0015C_{ab}^*$

Eq. 6. The k_L , k_C , and k_H values are the parametric factors, which are adjusted under different viewing parameters, for the lightness, chroma, and hue components, respectively. R_T function intends to improve the performance of the color difference equation for describing

chromatic differences in bluish colors.

$$\Delta E_{00} = \sqrt{\left(\frac{\Delta L^*}{K_L S_L}\right)^2 + \left(\frac{\Delta C_{ab}^*}{K_C S_C}\right)^2 + \left(\frac{\Delta H_{ab}^*}{K_H S_H}\right)^2} + R_T \left(\frac{\Delta C_{ab}^*}{K_C S_C}\right) \left(\frac{\Delta H_{ab}^*}{K_H S_H}\right) \quad \text{Eq. 5}$$

$$S_L = 1, S_C = 1 + 0.045 C_{ab}^*, \text{ and } S_H = 1 + 0.0015 C_{ab}^* \quad \text{Eq. 6}$$

Where

$\Delta L^*, \Delta C_{ab}^*, \Delta H_{ab}^*$: Differences of luminance, chroma, and hue

K_L, K_C, K_H : Parametric factors of luminance, chroma, and hue

S_L, S_C, S_H : Weighting function of luminance, chroma, and hue

R_T : Rotation function



2.4 Prior Color Breakup Suppression Methods

Color breakup phenomenon is a fatal drawback of FSC-LCDs. This phenomenon causes discomfort in human eyes and degrades image quality. Therefore, how to resolve the color breakup issue has been a major research in the FSC technique. Many color breakup suppression methods were proposed in different ways which can be categorized into motion compensation, inserting fields, and reducing color difference between sub-frames.

2.4.1 Motion compensation

The first part, motion compensation, was proposed to solve the dynamic color breakup. In Fig. 18, it shows the mechanism of motion compensation method [27]. This way is to display each field with a proper shift according to the moving velocity of the input image. After human eye integration, color breakup phenomenon caused by moving object can be

suppressed. However, if some minor objects having a chance to cross the observer's tracking path in the opposite direction, the perceived image of the crossing object would get worse than the conventional RGB driving method, as shown in Fig. 19.

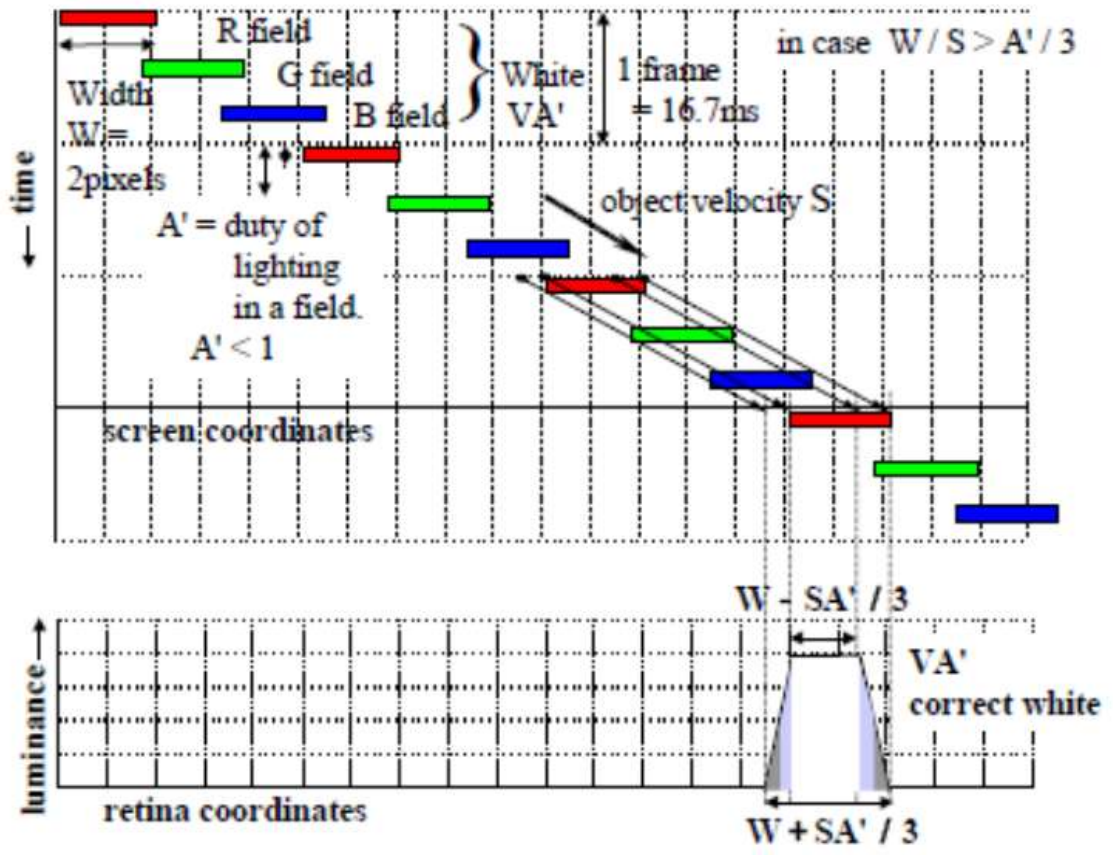


Fig. 18. The mechanism of motion compensation; color breakup was suppressed effectively.

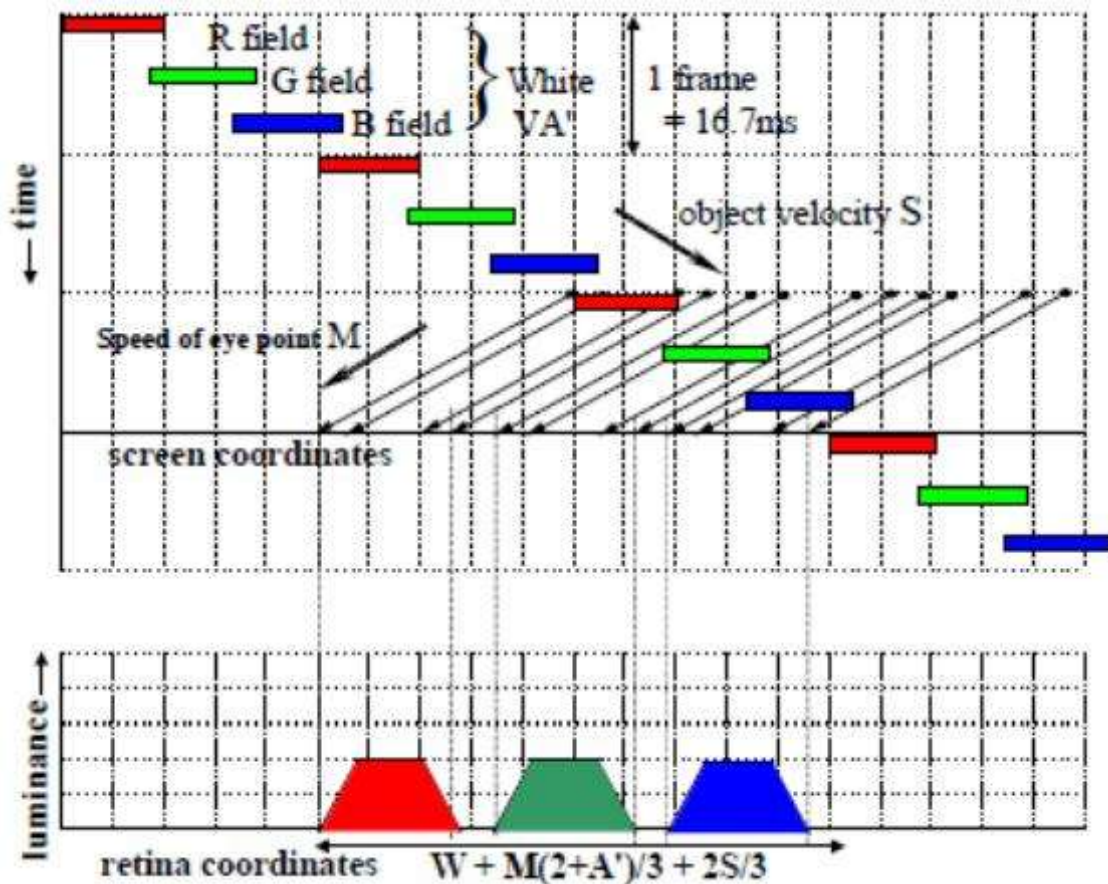


Fig. 19. The mechanism of motion compensation; object and observer's eye tracing path are in the opposite position.

2.4.2 Mono-color fields

In the second part, inserting fields, it can be further broken into two sections, mono-color fields and multi-color fields. Inserting mono-color fields is to increase the field rate up to 360Hz or higher, such as RGBRGB or RGBKKK [27][28]. By doing so, while there is eye movement, the width of separated color bars on the border of the displayed image would be reduced, as shown in Fig. 20. This method is often applied in the DLP projector with color wheel and digital micro-mirror-device (DMD). Moreover, inserting complementary color fields to the original three primary fields, such as RGBCY, is also useful due to decreasing the intensity of different colors. It can prevent observers from receiving the sensitive color of images as shown in Fig. 21. Nevertheless, inserting mono-color fields has to increase the field rate that challenges the current LC response time.

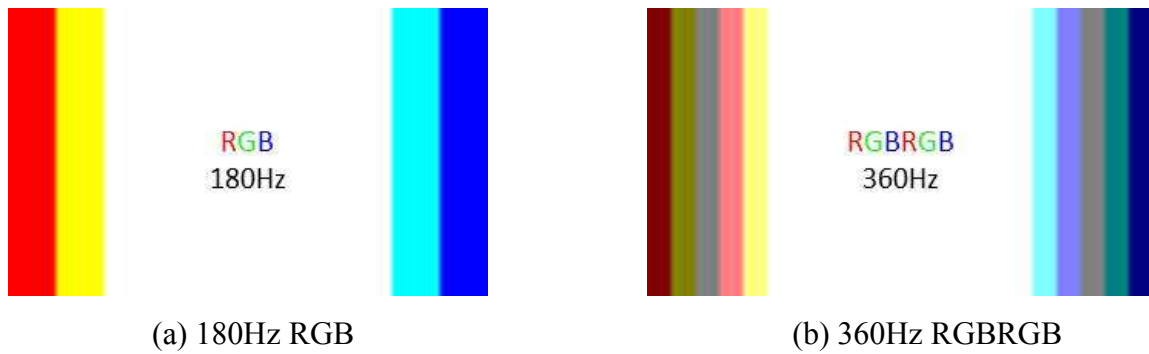


Fig. 20. Simulation color breakup image of (a) 180Hz RGB, and (b) 360Hz RGBRGB.

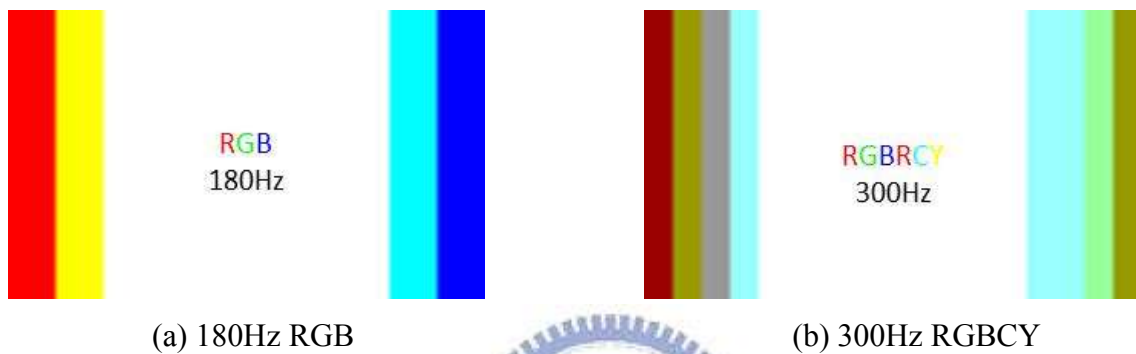


Fig. 21. Simulation color breakup image of (a) 180Hz RGB, and (b) 300Hz RGBCY.

2.4.3 Multi-color fields

The solutions mentioned above were proposed to effectively suppress color breakup, yet they are limited to be implemented on hardware by the strict LC response. In order to accomplish FSC method on hardware, the field rate must be lowered. Consequently, the Stencil-FSC methods [29]-[31] and the LPD method [32][33] with multi-color fields were proposed to make field rate lower than 240Hz and suppress color breakup effectively.

(a) Stencil-FSC methods

In Fig. 22, it shows the driving schemes of Stencil-FSC methods under different field rate. The main idea of Stencil-FSC method is to provide multi-color fields using locally controllable and dimmable backlight module. The 240Hz Stencil-FSC method is to display major information of input image with high luminance and rough color in the first field. Then

the other three fields show the detail of the remaining information in the three primary colors with lower luminance. Thus, luminance of the perceived separated color bars on the edge of the image would be concentrated in the first field, which means the color breakup phenomenon is effectively suppressed and almost imperceptible. In Fig. 23, we compare the color breakup phenomenon between conventional RGB driving method (Fig. 23(a)) and the 240Hz Stencil-FSC method (Fig. 23(b)).

The field rate of the 240Hz Stencil-FSC method is still a little higher than RGB driving method, so our team further proposed the 180Hz Stencil-FSC method to solve this issue. The concept of the 180Hz Stencil-FSC method is to combine the all green information with some parts of red and blue information in the first field. Then the rest of red and blue information are displayed in the second and the third field. This is due to human visual sensitivity acts stronger in the green color than in the other two primaries. In this regard, when color breakup comes up, the separated colors on the fringe do not contain green information so that the rainbow-like fringe can hardly be observed, as shown in Fig. 23(c).

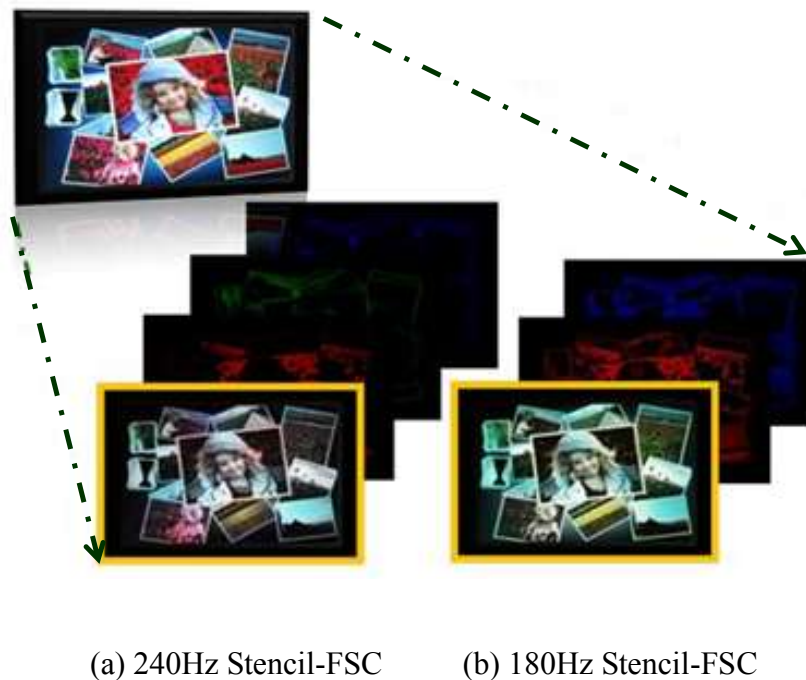
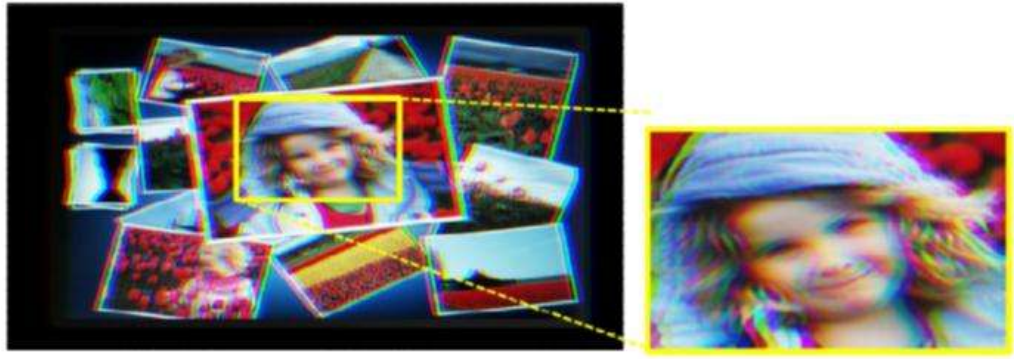


Fig. 22. The concept of Stencil-FSC methods: (a) 240Hz Stencil-FSC (b) 180Hz Stencil-FSC.



(a) Color breakup image of RGB-driving method with target image *Girl*.



(b) Color breakup image of 240Hz Stencil-FSC method with target image *Girl*.



(c) Color breakup image of the 180Hz Stencil-FSC method with target image *Girl*.

Fig. 23. Color breakup of image *Girl* by different FSC methods: (a) RGB-driving, (b) the 240Hz Stencil-FSC method.

(b) LPD method

The concept of LPD method is to redistribute the original three highly saturated primary-color backlight fields into less but sufficient ones, as shown in Fig. 24. In Fig. 24(b), the right hand side shows the three desaturated-primary-color fields, and Fig. 24(c) shows the reproduced image with color breakup phenomenon. Reducing color saturation can

lower the color difference between each two fields that the separated color would just be obtained as motion blur but not color breakup. To precisely reproduce an image as the target, the LPD method also utilizes the locally controllable backlight module as the Stencil-FSC methods. In the LPD method, the pixel chromaticity distribution of each backlight segment is analyzed in the CIE1976 $u'v'$ uniform color space, as Fig. 25 shows. By doing so, the colors of the three backlight fields are desaturated by mixing other colors in the same field that the color breakup was significantly reduced.

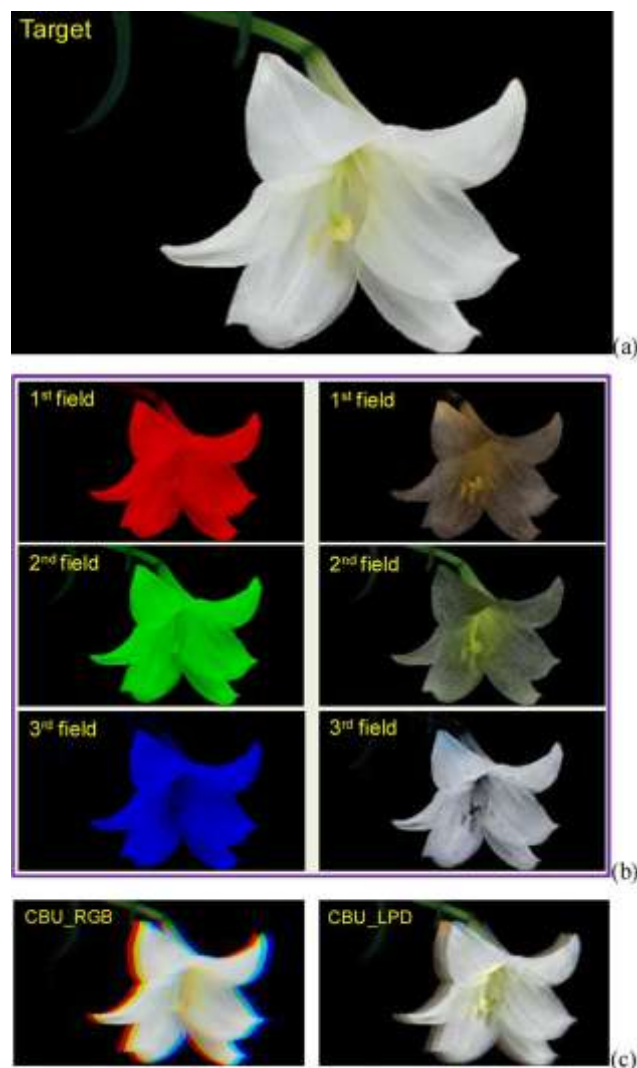


Fig. 24. The concept of LPD method. (a)The target image, *lily*. (b)The three fields of RGB driving (left) and the LPD method (right). (c)Color breakup simulation with 15 pixels shifted for each field using RGB driving (left) and the LPD method (right) [32][33].

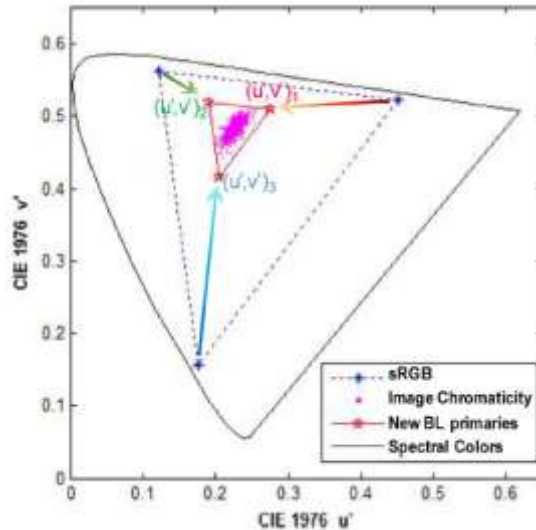


Fig. 25. The triangles represent color saturation of sRGB and LPD backlight primary-colors in the CIE1976 $u'v'$ uniform color space.

(c) Two-field methods

The 180Hz methods can be implemented on the OCB mode of LC displays but still not enough for large size or commercial LC modes. Accordingly, the two-field method with two color filters (2F2CF) and the 120Hz two-color-field method were proposed to be applied to any mode of commercial LC and any size of LCDs.

A spatial-temporal display method, which has 2 fields and 2 color filters that is called 2F2CF method, was proposed to enhance image quality of displays [12][13]. This method combined spatial color mixing with color filters and temporal color mixing with sequential backlight flashing. Each pixel has two sub-pixels with two different color filters and two fields with different backlight colors. The idea of 2F2CF method with two typical types is illustrated in Fig. 26 and Fig. 27 [12]. By changing the spectra of the color filters and backlights, different color combinations can be achieved.

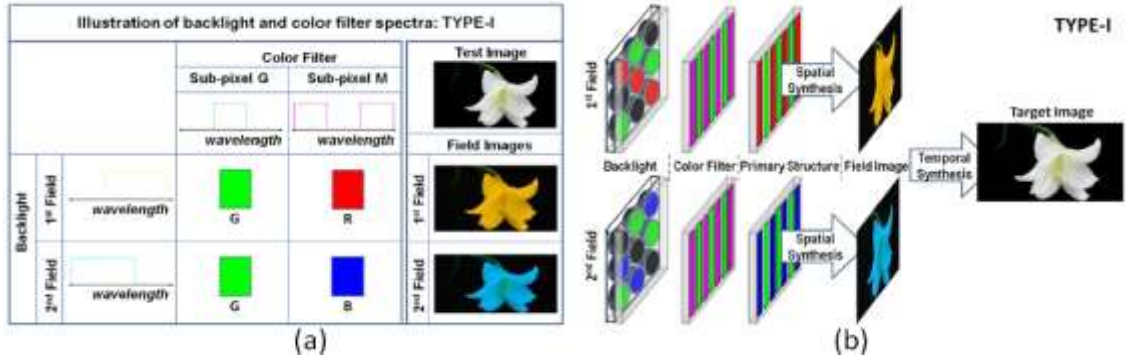


Fig. 26. A 2F2CF type with yellow-cyan (Y-C) backlights and green-magenta (G-M) color filters. (a)Spectrum-level illustration for the color synthesis procedure. (b)The configuration of type-I 2F2CF LCD.

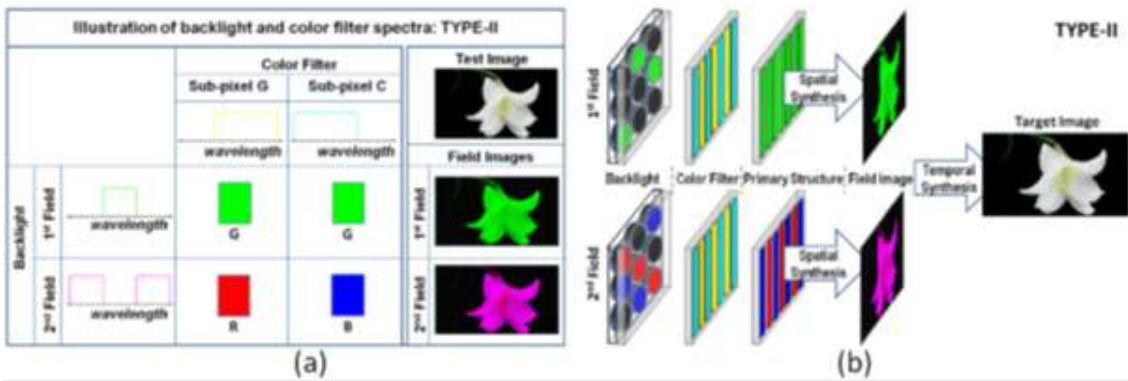


Fig. 27. Another 2F2CF type with green-magenta (G-M) backlights and yellow-cyan (Y-C) color filters. (a)Spectrum-level illustration for the color synthesis procedure. (b)The configuration of type-II 2F2CF LCD.

Though the 2F2CF method can accurately reproduce an image as the target, it still needs color filters, which would lower luminance and spatial resolution. Consequently the two-color-field method was proposed without color filter. The thought of two-color-field method is to divide the primary color with the least information into two parts. The divided parts are then combined with the other two primary color fields to serve as backlight signals, as shown in Fig. 28 [11]. However, serious image distortion would be generated in this way because a part of image colors would not be displayed, i.e., the blue dots far from the red line as shown in Fig. 29. Besides, the two-color-field method utilized the primaries on the maximum display gamut as the red points shown in Fig. 29(b), which would suppress color breakup limitedly.

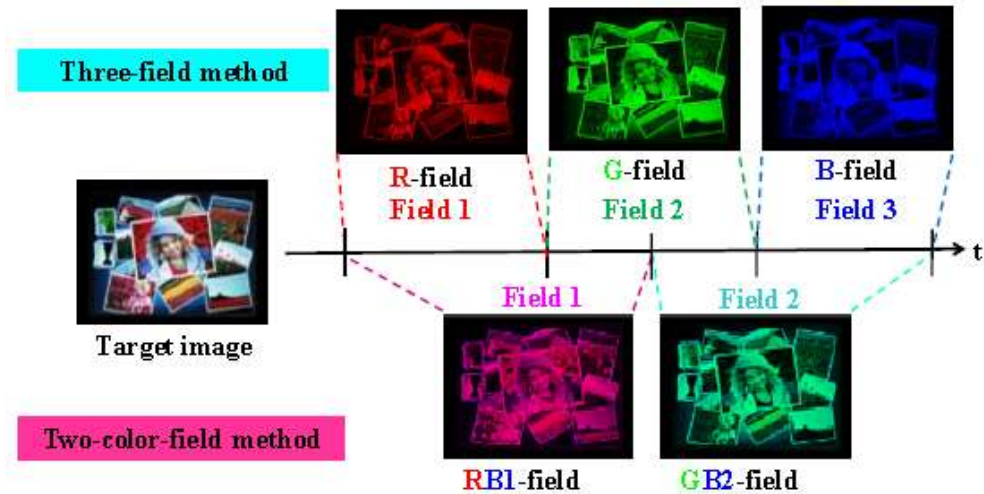


Fig. 28. Two driving schemes, a 180Hz RGB driving type and the two-color-field method. By field decomposition of color fields to form full-color image.

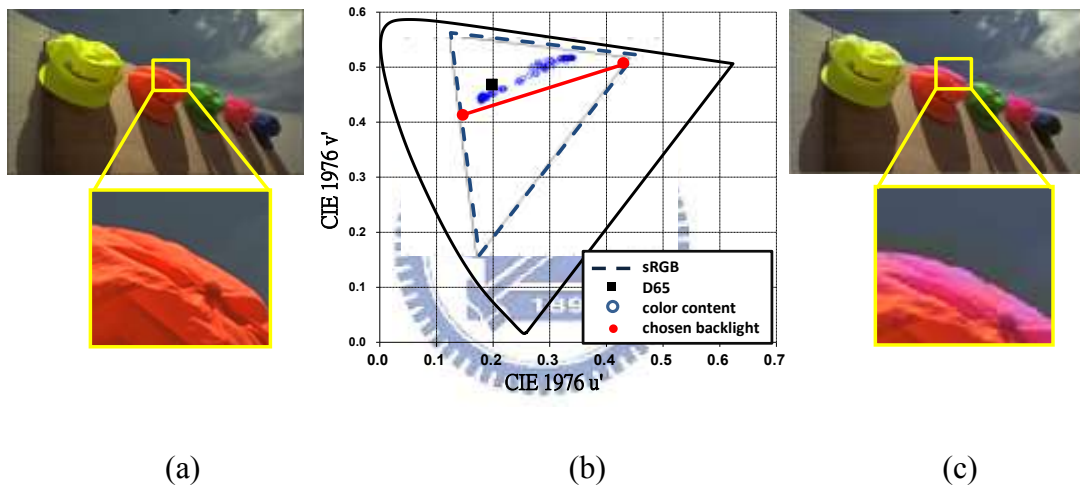


Fig. 29. (a) A test image and one of backlight segments with its (b) pixel chromaticity distribution (blue circles) and the backlight chromaticity of two fields (red dots) in the CIE1976 $u'v'$ color space. (c) The reproduced distorted image using the two-color-field FSC method [11].

2.5 Summary

The accompaniment of FSC-LCDs, color breakup, is perceived when a relative velocity happens between human eyes and displayed object. Several solutions were proposed to suppress this phenomenon. However, these methods are too hard to be implemented on hardware with large size, even the 180Hz Stencil-FSC method. Two 120Hz methods,

spatial-temporal method (2F2CF) and two-color-field method were also proposed considering slow LC response. Some issues come up with these two methods such as lower light transmission than conventional FSC-LCDs in the 2F2CF method, and color distortion in the two-color-field method. Therefore, the 120Hz Stencil-LPD method is proposed under a low field rate, 120Hz, to keep image quality without color filter, and to suppress color breakup.



Chapter 3

120Hz Stencil-LPD Method

A two-field driving scheme lacks the third temporal degree of freedom in displaying the third primary information, which would cause distortion upon absent information. Consequently, we apply spatially adjustable color backlight into a two-field FSC LCD to substitute the color filter. By doing so, image fidelity would be raised due to suitable backlight signals. Hence, many commercial LC modes such as TN, IPS, and MVA modes can achieve the response time since the field rate maintained at 120Hz. The backlight determination method and the corresponding algorithm will be described below.

3.1 Concept

The concept of the proposed backlight determination method comes from the idea of Stencil-FSC method and the local primary desaturation (LPD) method. Apparent from previous two-field FSC LCDs, which utilize the primaries on the maximum display gamut, we select the backlight signals according to color content in each backlight segment. Different from LPD, the proposed method shows the most represented colors instead of the desaturated primaries, as shown in Fig. 30. By doing so, multiple colors with majority color information instead of mono color are displayed in a single field without color filters. Less color information would be lost using the 120Hz Stencil-LPD compared to the previous two-color-field method, as Fig. 31 shows.

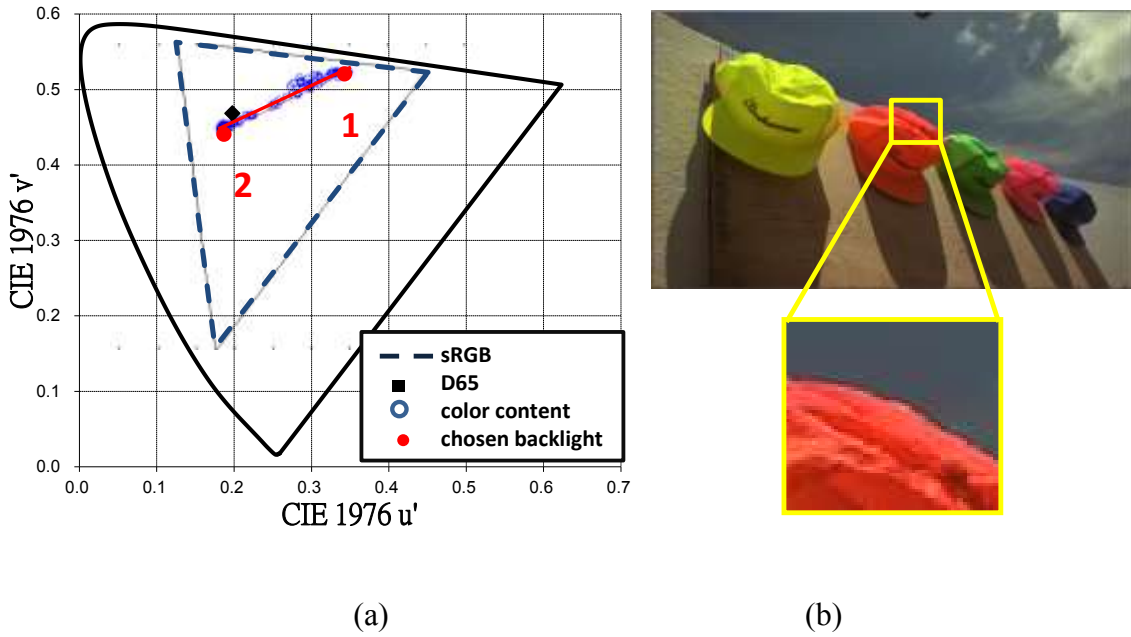


Fig. 30. The concept of proposed Stencil-LPD method with (a) pixel chromaticity distribution in one of backlight segments in (b) the test image. According to the color distribution tendency (blue dots), we choose the backlight signals (red dots 1 and 2) for two fields in each segment.

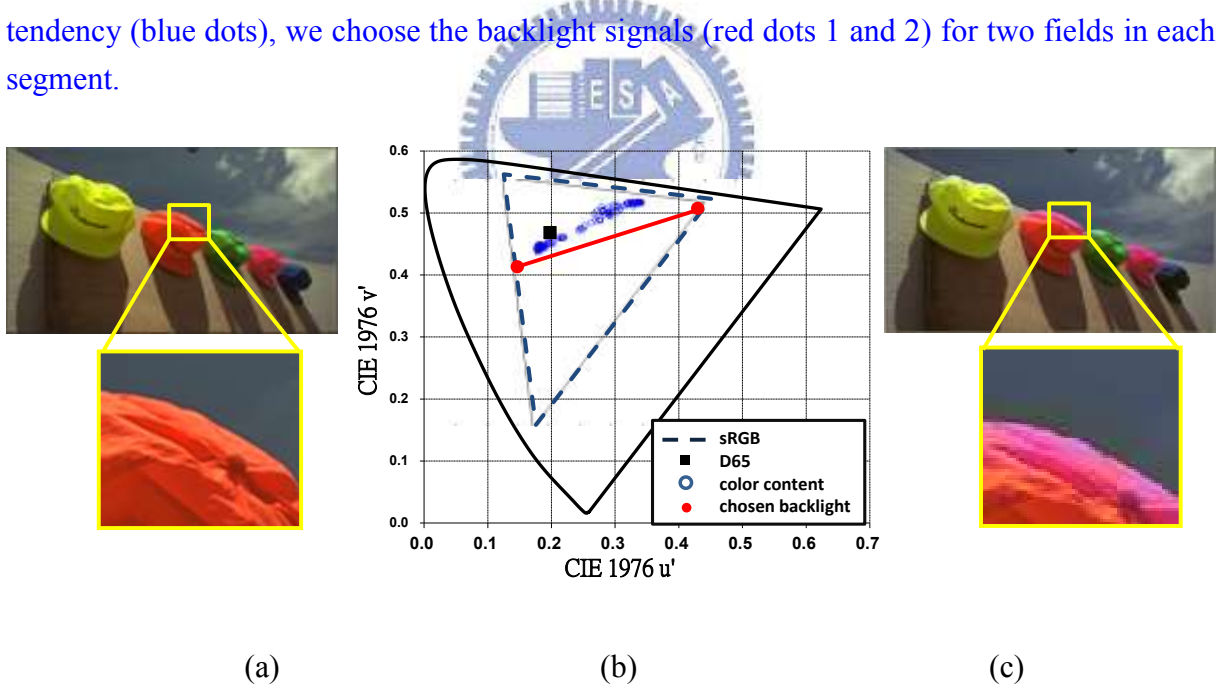


Fig. 31. (a) A test image and one of backlight segments with its (b) pixel chromaticity distribution (blue circles) and the backlight chromaticity of two fields (red dots) in the CIE1976 $u'v'$ color space. (c) The reproduced distorted image using the two-color-field FSC method.

3.2 Algorithm

The flow chart of the Stencil-LPD method is shown in Fig. 32. In this thesis, all the input image signals are first transferred from sRGB, $(RGB)_o$, (gamma is 2.2 with D65 as white point) to tri-stimulus values in the CIEXYZ color space as target signals, $(XYZ)_o$, according to

$$\begin{bmatrix} X \\ Y \\ Z \end{bmatrix} = \begin{bmatrix} 0.4124 & 0.3576 & 0.1805 \\ 0.2126 & 0.7152 & 0.0722 \\ 0.0193 & 0.1192 & 0.9505 \end{bmatrix} \begin{bmatrix} R_{linear} \\ G_{linear} \\ B_{linear} \end{bmatrix} \quad \text{Eq. 7.}$$

The algorithm is then divided into two parts: backlight determination and LC calculation. Details of both parts will be elaborated in this section.

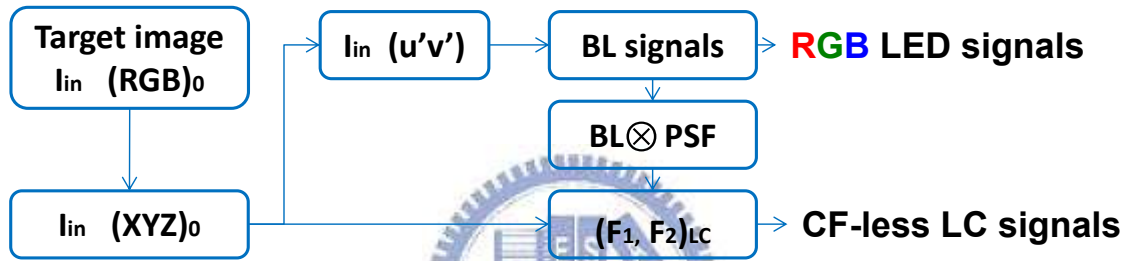


Fig. 32. Flow chart of Stencil-LPD method.

$$C_{linear} = \begin{cases} \frac{C_{srgb}}{12.92} & , C_{srgb} \leq 0.04045 \\ \left(\frac{C_{srgb} + 0.055}{1.055} \right)^{2.4} & , C_{srgb} \geq 0.04045 \end{cases} \quad , \text{ where } C \text{ is } R, G, \text{ or } B.$$

$$\begin{bmatrix} X \\ Y \\ Z \end{bmatrix} = \begin{bmatrix} 0.4124 & 0.3576 & 0.1805 \\ 0.2126 & 0.7152 & 0.0722 \\ 0.0193 & 0.1192 & 0.9505 \end{bmatrix} \begin{bmatrix} R_{linear} \\ G_{linear} \\ B_{linear} \end{bmatrix} \quad \text{Eq. 7}$$

3.2.1 Backlight determination

To determine the represented colors as backlight signals, the pixel chromaticity distribution in each backlight segment were further analyzed in the CIE1976 $u'v'$ uniform color space. The chromaticity of every pixel was plotted on the CIE1976 $u'v'$ colors diagram as Fig. 30(a) shows. Therefore, the trend of distribution can be obtained. Since the tendency of the color content has been found according to the regression formula in *where*

$$m = \frac{\sum_{i=1}^n (u'_i - \bar{u}') (v'_i - \bar{v}')}{\sum_{i=1}^n (u'_i - \bar{u}')^2}, \quad \text{and } c = \bar{v}' - m \times \bar{u}' \quad \text{Eq. 8, the}$$

two most represented colors are determined as backlight signals in a single segment. The chromaticity of each pixel here is seen as a coordinate set, (u, v), on the colors diagram, and the regression line is regarded as L. Colors along the connected line between the two chosen colors (point 1 and point 2) can now be displayed.

$$\bar{u}' = \frac{\sum_{i=1}^n u'_i}{n}, \quad \bar{v}' = \frac{\sum_{i=1}^n v'_i}{n}$$

$$L: m \times u' + v' - c = 0,$$

$$\text{where } m = \frac{\sum_{i=1}^n (u'_i - \bar{u}') (v'_i - \bar{v}')}{\sum_{i=1}^n (u'_i - \bar{u}')^2}, \quad \text{and } c = \bar{v}' - m \times \bar{u}' \quad \text{Eq. 8}$$

Besides, after choosing two colors as backlight signal in each segment, how to divide the two signals of the two fields is also a key factor in image quality. As shown in Fig. 33, we first regard the most appeared color of each segment as the first field signal and the less one in the second field. We can discover that some obvious lines would come up by the edge of a sudden change of colors. To avoid the unexpected and annoying lines, we now adjust the colors and put similar colors into the same field to make the changes more gradual. By doing so, we can see that the unwanted lines disappeared and the image quality gets better, as shown in Fig. 33(b).

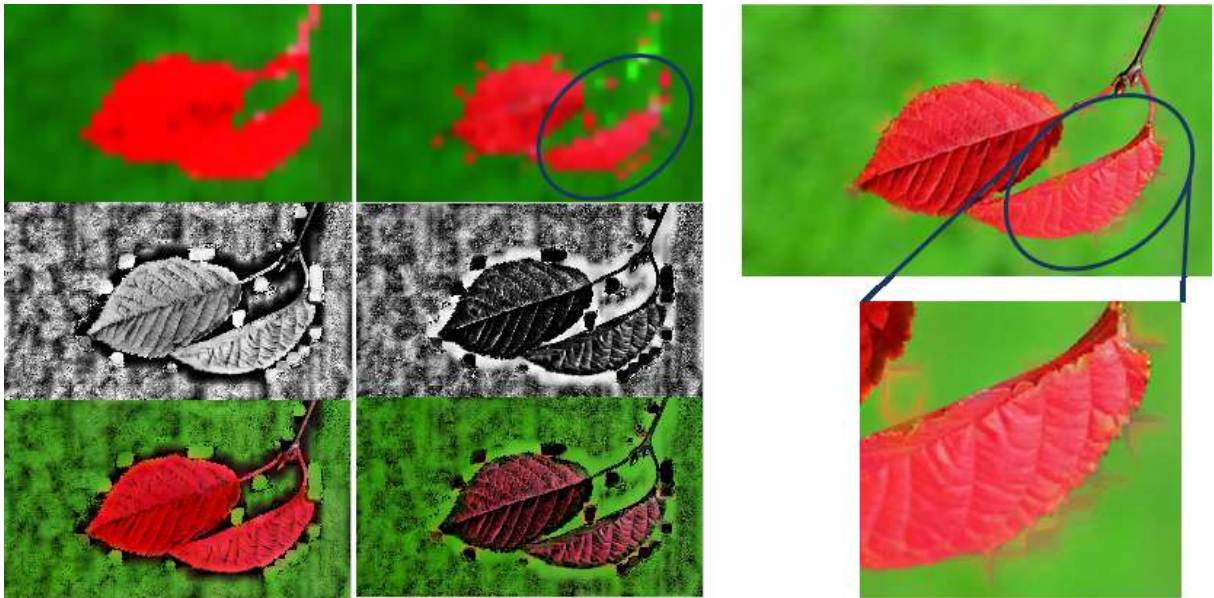


Fig. 33(a) The most represented color of each segment in the first field (up) with compensated LC signals (middle) causes annoying lines.



Fig. 33(b) Similar colors in the same field reduces the annoying lines.

3.2.2 LC calculation

The signals of RGB-LED backlight and LC are computed by transferring the input image signals to tri-stimulus values in CIEXYZ color space as target signals. On the other hand, the backlight signals are also transferred to CIEXYZ color space after calculating the backlight

intensity distribution. The relation among the target ($X_0, Y_0,$ and Z_0), backlight contribution $((XYZ)_1, (XYZ)_2)$, and the LC signals (F_1, F_2) of the two fields are shown in

$$\Rightarrow \begin{bmatrix} F_1 \\ F_2 \end{bmatrix}_{LC} = \begin{bmatrix} X_1 & X_2 \\ Y_1 & Y_2 \\ Z_1 & Z_2 \end{bmatrix}_{BL}^{-1} * \begin{bmatrix} X_0 \\ Y_0 \\ Z_0 \end{bmatrix}_{Target} \quad \text{Eq. 9.}$$

Notice that when we calculate the LC signals, there is no inverse matrix for the tri-stimulus of backlight distribution in linear algebra here because it is a 3 by 2 matrix. Hence, here we use the least square to find the LC signals with minimum errors.

$$\begin{bmatrix} X_0 \\ Y_0 \\ Z_0 \end{bmatrix}_{Target} = \begin{bmatrix} X_1 & X_2 \\ Y_1 & Y_2 \\ Z_1 & Z_2 \end{bmatrix}_{BL} * \begin{bmatrix} F_1 \\ F_2 \end{bmatrix}_{LC}$$

$$\Rightarrow \begin{bmatrix} F_1 \\ F_2 \end{bmatrix}_{LC} = \begin{bmatrix} X_1 & X_2 \\ Y_1 & Y_2 \\ Z_1 & Z_2 \end{bmatrix}_{BL}^{-1} * \begin{bmatrix} X_0 \\ Y_0 \\ Z_0 \end{bmatrix}_{Target} \quad \text{Eq. 9}$$

We can see that because of the 3 by 2 matrix, there might not be an exact set of solution for the three equations with two variables. Though the least square optimization is applied to solve this problem, considering that LC signals are limited from zero to one, the best solution found by the least square optimization might be illegal. Therefore, an approximating way is employed when the solution is beyond zero to one to get the most suitable solution. The diagram of this approximation is illustrated in Fig. 34. The core of the approximation is to divide the range of zero to one evenly into ten parts and to locate where the least error happens. After the region of the least error is found, we then divide this region into ten parts equally again and repeat the same procedure.

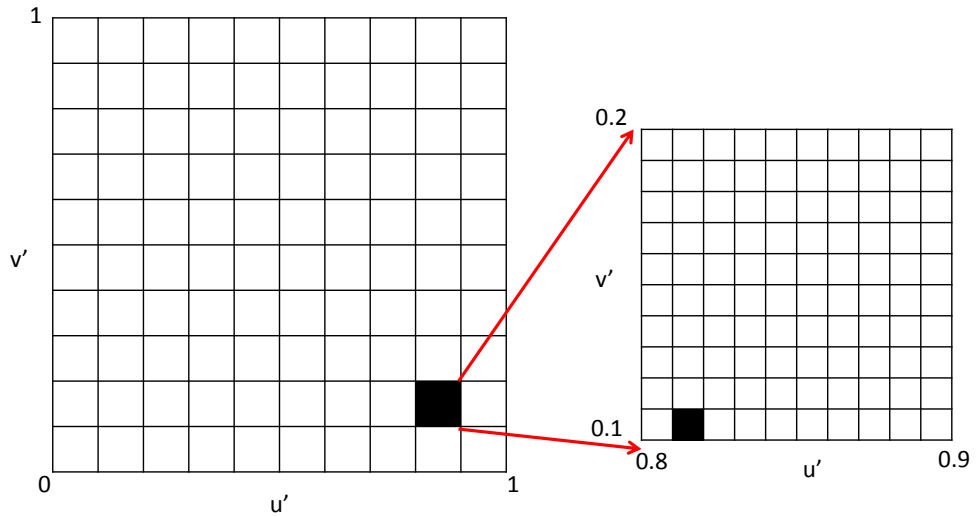


Fig. 34. The approximation method.

After the backlight and LC signals are determined, the reproduced image can be displayed with less distortion and color breakup. With this Stencil-LPD method, the backlight module provided a proper and reduced but sufficient saturated backlight color and modulated the LC signals to maintain image detail as shown in Fig. 35.

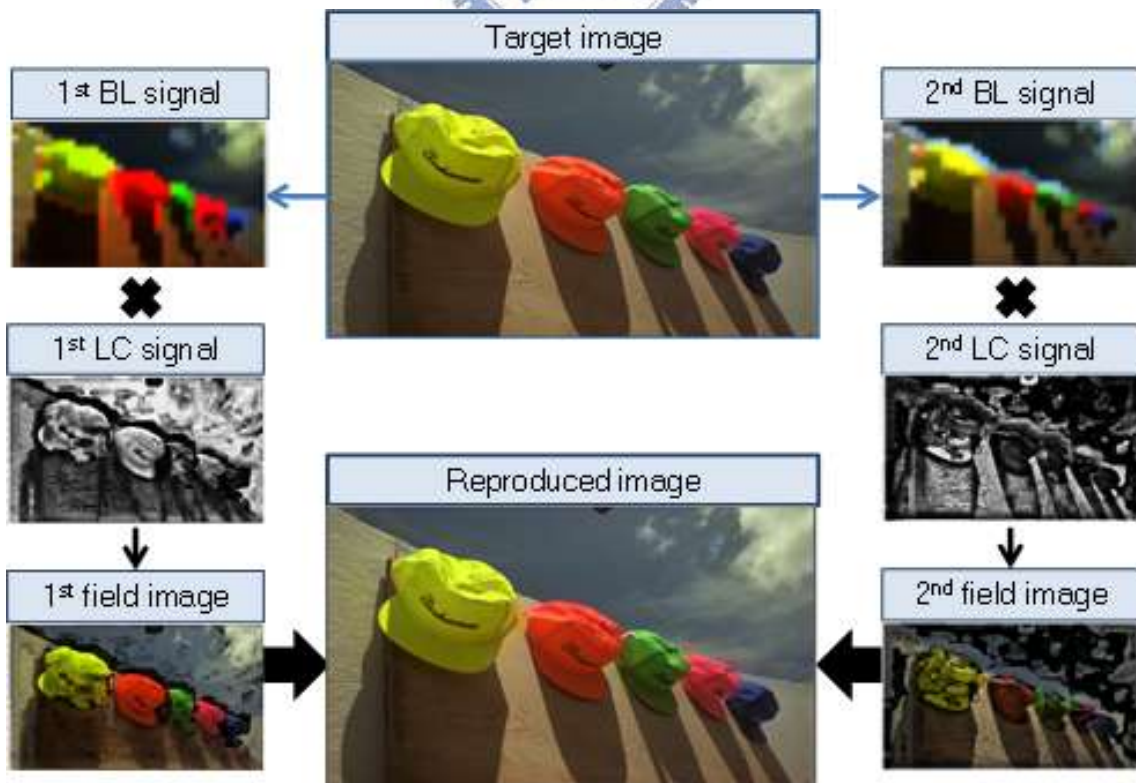


Fig. 35. The driving scheme of Stencil-LPD method.

3.3 Simulation results

To first verify the proposed method, we choose 9 different images that the color saturation and image complexity vary from one to another, as shown in Fig. 36. In the simulation, the backlight division of 32*24, and the image resolution of 1920*1080 were assumed. We use CIEDE2000 (ΔE_{00}), which the criteria of acceptable is 3, as the scale to estimate color difference.

Based on the CIEDE2000, the pixel distortion ratio, PDR ($\Delta E_{00} > 3$) index, defined by

$$\text{PDR}(\Delta E_{00} > 3) = \frac{\text{\# of } \Delta E_{00} > 3 \text{ pixels}}{\text{\# of total pixels}} \times 100\% \quad \text{Eq. 10,}$$

is applied as an index to judge the image fidelity. Besides, the relative CBU, defined by

$$\text{where } a, b \text{ are the backlight division number} \quad \text{Eq. 11,}$$

is computed to decide how serious the CBU is. These two indices are employed here to compare the Stencil-LPD method with the prior two-color-field method.

In the simulation results, both PDR and the relative CBU values are lower in the Stencil-LPD method than in two-color-field method. The color breakup is simulated by moving 20 pixels in each field.



Fig. 36. Nine test images varying in color saturation and image complexity: Lily, Finger, Polar bear*, Red leaf, Hats, Plane, Teapot#, Sashimi, and Basketball.

(*: provided by Taiwan Tourism Bureau, <http://tiscsvr.tbrc.gov.tw>, #: taken by Jens Rubbert, http://jensru.jalbum.net/Jens_Rubbert).

$$PDR(\Delta E_{00} > 3) = \frac{\# \text{ of } \Delta E_{00} > 3 \text{ pixels}}{\# \text{ of total pixels}} \times 100\% \quad \text{Eq. 10}$$

$$\text{relative CBU} \equiv \frac{\sum \Delta E_{00}(\text{120Hz driving})_{a,b}}{\sum \Delta E_{00}(\text{180Hz RGB driving})} \times 100\%,$$

where a, b are the backlight division number Eq. 11

The 120Hz Stencil-LPD method enhances the image fidelity by choosing the proper colors as backlight signals to decrease the lost information. The simulation results are summarized in Fig. 37. The average $PDR(\Delta E_{00} > 3)$ is about 21.4%, reduced to 52.3% compared to the two-color-field FSC method. Additionally, the 120Hz Stencil-LPD method also has better performance in color breakup suppression. The color saturation is reduced to the exact point where it meets the image requirement but not affecting the quality of the images in each backlight segment. By using the proposed 120Hz Stencil-LPD method, less difference between

the two fields would be observed, makes color breakup effectively suppressed. Fig. 38 and Fig. 39 show the reproduced images using 120Hz Stencil-LPD and the two-color-field FSC methods with color difference images.

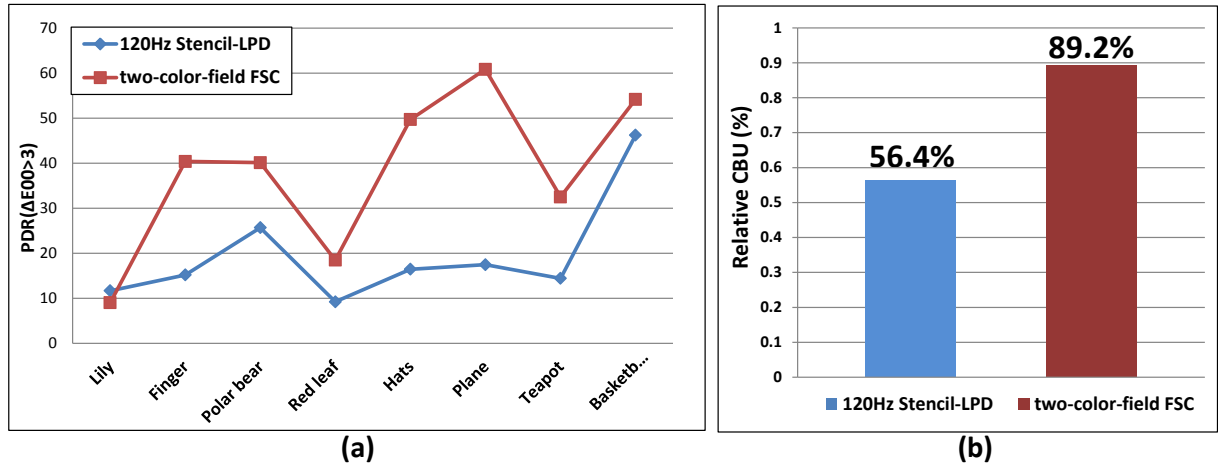


Fig. 37. (a) The PDR ($\Delta E_{00} > 3$) values of nine test images in the two methods and (b) the relative CBU.

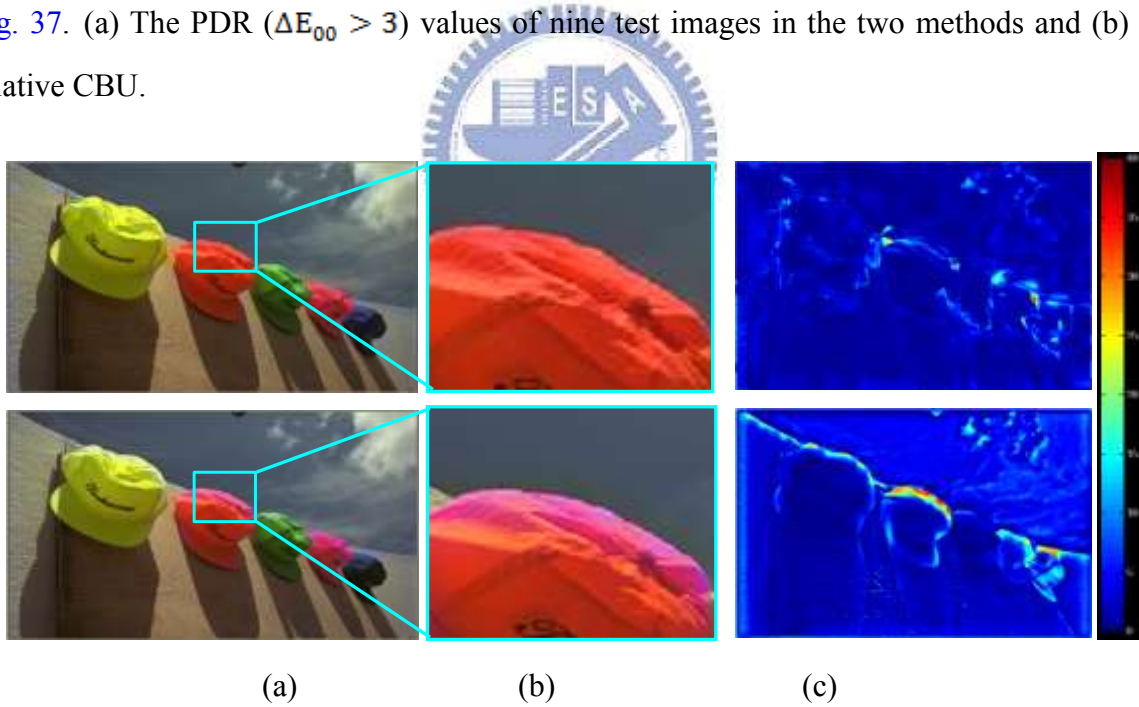


Fig. 38. Hats: (a) The reproduced images and (b) the color difference images by the 120Hz Stencil-LPD (up) and two-color-field FSC methods (down).

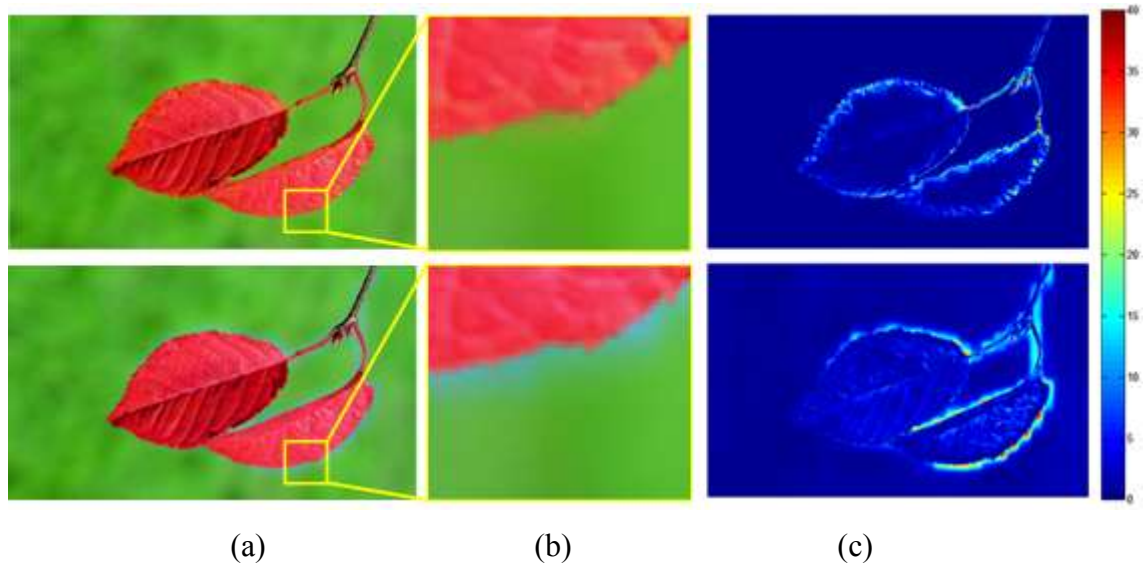


Fig. 39. Red leaf: (a) The reproduced images and (b) the color difference images by the 120Hz Stencil-LPD (up) and two-color-field FSC methods (down).

3.4 Discussion

Though the 120Hz Stencil-LPD method has enhanced the image fidelity, there might still be some issues. As mentioned at the beginning of this chapter, a two-field driving scheme lacks the third degree of freedom to display all the information, the same disadvantage exists in the 120Hz Stencil-LPD method. As Fig. 40 shows, when there is too many image content in one segment, some colors could not be displayed so some distortion happens.

To solve this problem, the best way is to increase the number of backlight division so the content of each segment can be reduced. However, gaining the number of backlight division increases the cost and computation complexity. Considering the tradeoff between image quality and the cost on hardware, the number of backlight division must be optimized.

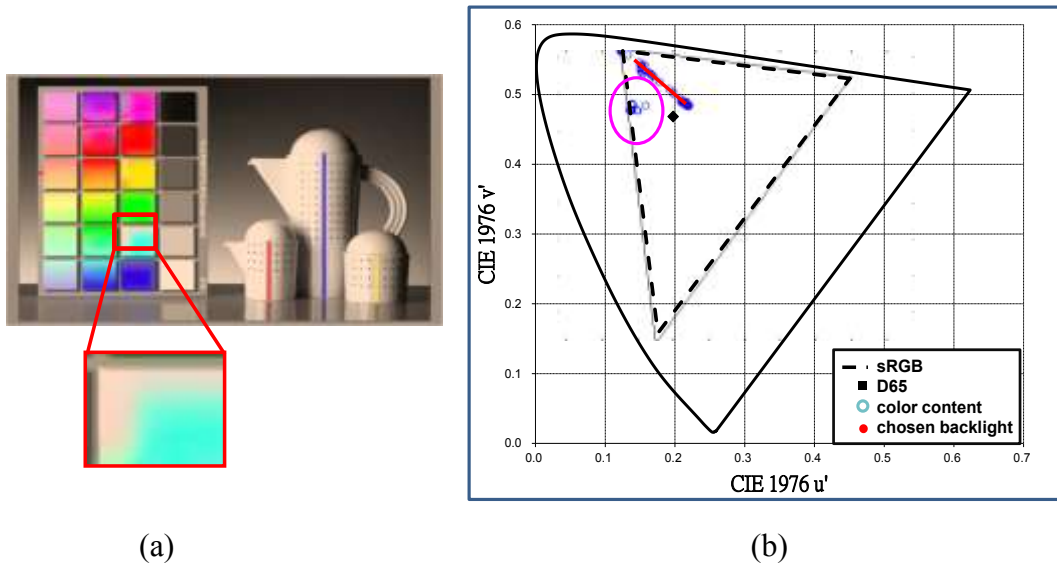


Fig. 40. (a) The distortion happens when there is too many color content in one segment. (b) The chromaticity distribution (blue dots) and the absent information that could not be displayed (in the green circle).

3.5 Summary

The two-color-field method can lower field rate of FSC-LCDs to only 120Hz without color filter. However, it has the drawback of image quality comes from absent color information. Thus, we proposed the Stencil-LPD method to enhance the image quality by applying proper backlight signals according to the image content. Some distortion would happen still because there is too many color content in one segment. In next chapter, the number of backlight division will be optimized.

Chapter 4

Optimization and Simulation Results

To reduce the error of colorimetric reproduction in images with complex content, the number of backlight segment must be modified. Then the results of image fidelity and color breakup suppression will be presented. Finally, we will verify the simulation results on a 46-inch MVA LCD.

4.1 Backlight Division Optimization

Ten images with different image content were chosen as test image as shown in Fig. 41. We verify the best backlight division with the indices such as $PDR(\Delta E_{00} > 3)$ and average power representing the image fidelity and power consumption individually. The index, $PDR(\Delta E_{00} > 3)$, pixel distortion ratio, is defined in

$$PDR(\Delta E_{00} > 3) = \frac{\# \text{ of } \Delta E_{00} > 3 \text{ pixels}}{\# \text{ of total pixels}} \times 100\%$$

Eq. 10. The

results, as shown in Fig. 42, show that as the number of backlight segment increases, color difference of test images decreases. It means the more independent backlight segments, the higher resolution of output backlight distribution would be provided. It is more adequate to be compensated by the LC module. Also, in this way, the backlight signals could be more accurate because of less color content is included. The backlight division of 64*36 is the optimized value since color difference only varies slightly exceeding this value.



Fig. 41. Ten test images with different image content.

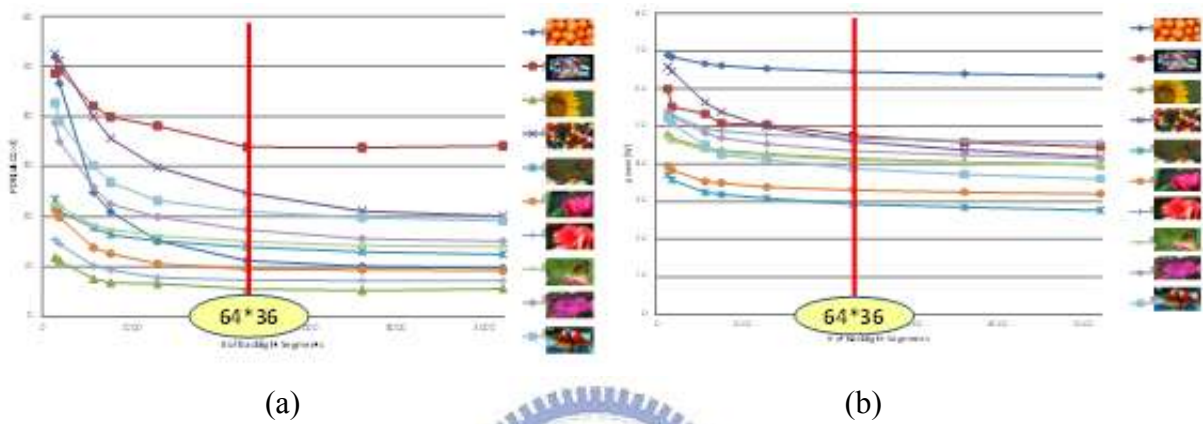


Fig. 42. The simulation results with indices (a) $PDR(\Delta E_{00} > 3)$ and (b) power.

4.2 Results

The backlight segment optimization was accomplished in the previous section. The reproduced images with optimal results are presented below. Also, color difference maps are applied to evaluate colorimetric reproduction accuracy. Finally, demonstration results will be given.

4.2.1 Color Difference Maps

Color difference maps were applied to evaluate the accuracy of colorimetric reproductions, using CIEDE2000 as the evaluation index. The three test images, (a)Teapot, (b)Girl, and (c)Sunflower, differ in either image details and color saturation are shown in Fig. 43. The optimal results simulated by Matlab, are illustrated in Fig. 44. Comparing the optimal reproduced images using Stencil-LPD method with the target images, human eye can hardly observe the color difference while comparing with the reproduced images utilizing the

two-color-field method. Besides, the average CIEDE2000 value in the reproduced Teapot image is only 0.82 and the $PDR(\Delta E_{00} > 3)$ value is 7.61% of the Stencil-LPD method while they are 4.48 and 61.4% individually in 2-color-field method. Though the average CIEDE2000 value of the reproduced Girl image is 3.37 that it is distinguishable, the image content is so complicated that human eye can still hardly see the color difference. Similarly, the results of the Sunflower image show that with the Stencil-LPD method, the difference between the target image and the reproduced image is almost invisible.

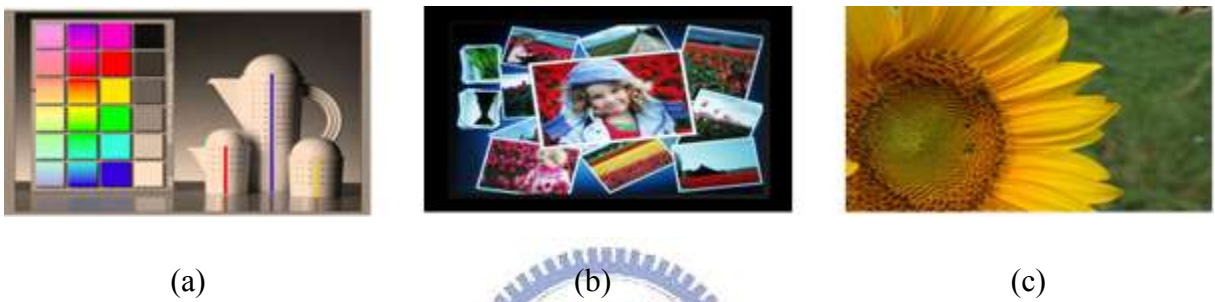
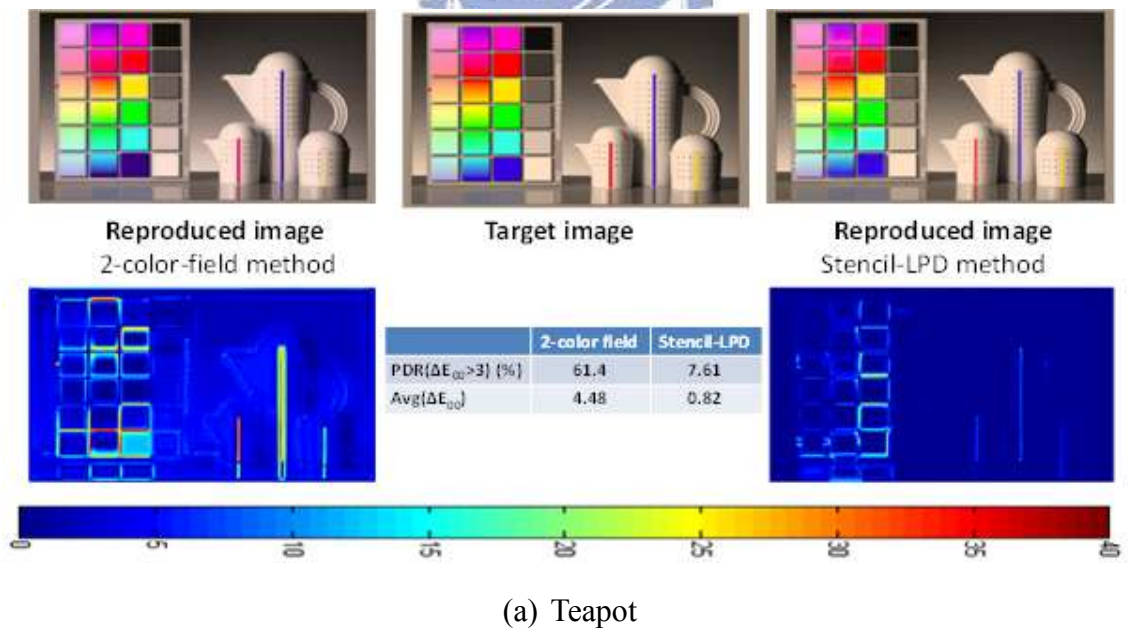
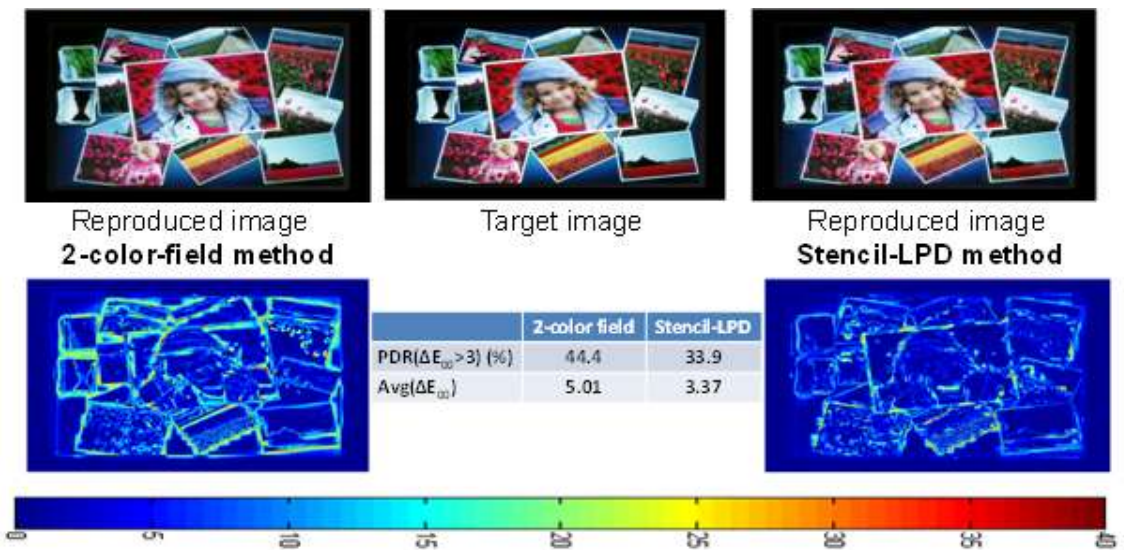
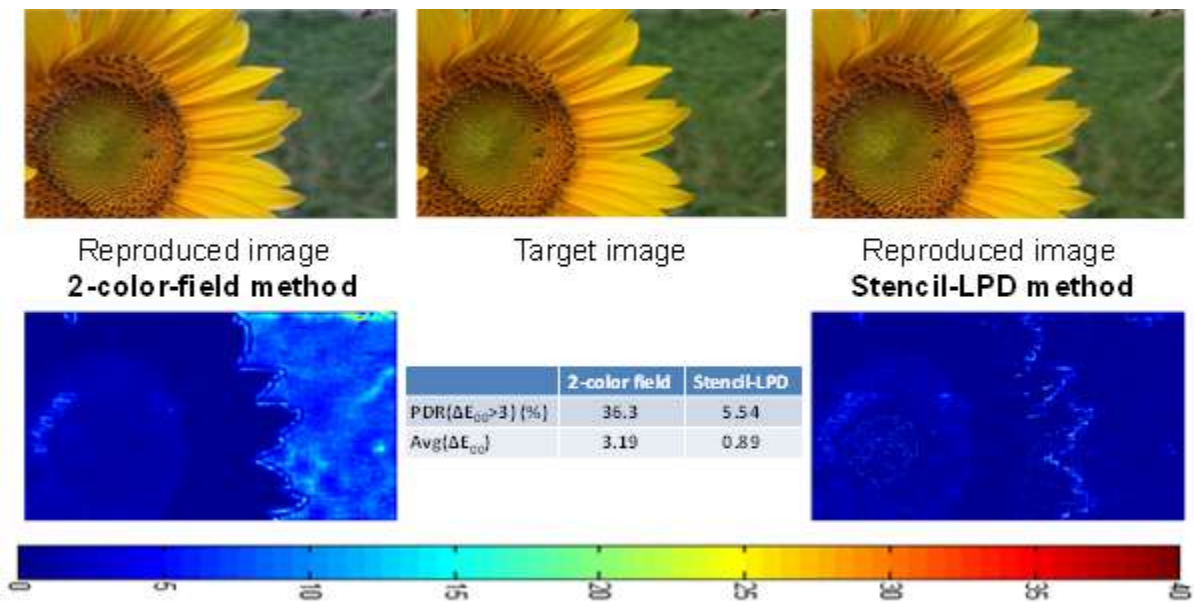


Fig. 43. Three test images: (a) Teapot, (b) Girl, and (c) Sunflower.





(b) Girl



(c) Sunflower

Fig. 44. The reproduction results of the three test images.

4.2.2 Demonstration Results

A 46-inch 120Hz MVA LCD were used to demonstrate the CBU suppression results. The CBU visibility was compared between two reproduced images by the 2-color-field and the Stencil-LPD methods. A camera moved horizontally to simulate the eye movement in capturing CBU images. The reproduced images using the 2-color-field and the Stencil-LPD

methods are shown in Fig. 45. In Fig. 46, the color fringes of the color checker induced by (a) mixed colors (red with partial blue and green with remaining partial blue), are obvious while the fringe seems like motion blur (b) using the Stencil-LPD method. The Stencil-LPD method provides a less but sufficient color saturation so the difference between the two field images is little that makes less CBU observation.

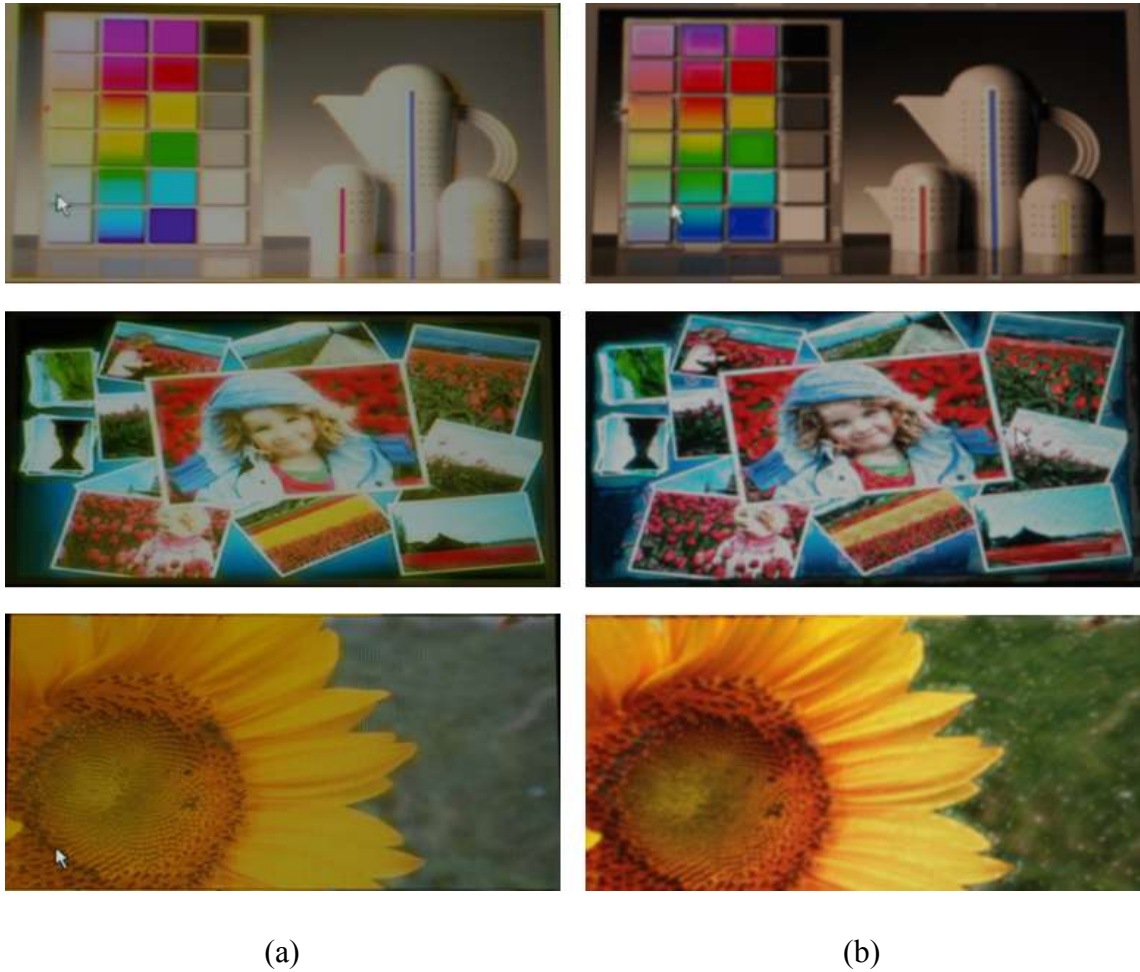


Fig. 45. The reproduced images with (a) 2-color-field method and (b) Stencil-LPD method

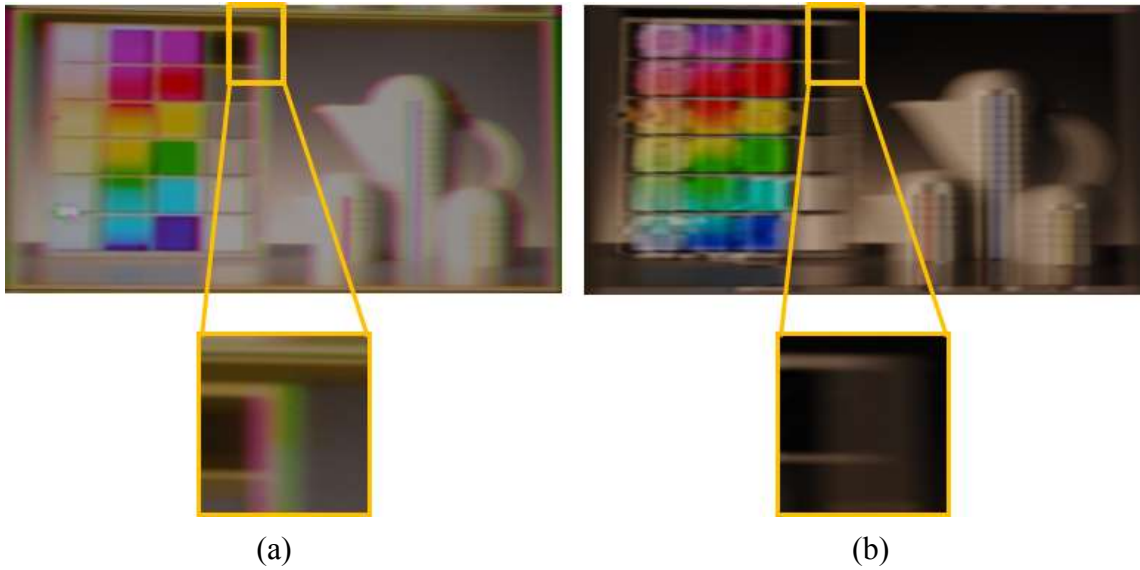


Fig. 46. The CBU images by shaking the camera horizontally to simulate eye movement with (a) 2-color-field method and (b) Stencil-LPD method.

4.3 Comparison

A comparison of the proposed method and other methods are shown in Table 1. The Stencil-LPD method has some advantages like color filter free, three times of luminance and spatial resolution, low field rate with 120Hz and only 2 fields. The experimental results show that the Stencil-LPD method not only reduces the color difference but also suppresses CBU effectively with locally backlight controlling technology.

Table 1. Comparison of NCTU Stencil-LPD method and other FSC methods

| | Conventional LCDs | RGB Driving | 2F2CF | Two-color-field FSC | 120Hz Stencil-LPD |
|-------------------------------------|-------------------|--------------|------------|---------------------|-------------------|
| | | Samsung, CPT | Philips | NCTU | |
| Optical throughput | 1x | 3x | 1.5x | 3x | 3x |
| Resolution | 1x | 3x | 1.5x | 3x | 3x |
| Color filter | 3 | 0 | 2 | 0 | 0 |
| Field rate (Hz) | 60 | 180 | 120 | 120 | 120 |
| Fidelity PDR($\Delta E_{00} > 3$) | 0 | 0 | 0 | 38.2% | 18.3% |
| Color breakup | | Serious | Acceptable | Acceptable | Imperceptible |

4.4 Summary

Optimization of the Stencil-LPD method was completed in this chapter. The colorimetric reproduction with the optimal backlight divisions was much lower in the average of CIEDE2000 and $PDR(\Delta E_{00} > 3)$ value compared with the 2-color-field method. Besides, the demonstrated results show the well-suppressed CBU visibility.



Chapter 5

Conclusion and Future Works

5.1 Conclusion

Differ from the conventional LCDs, the color filter-less FSC LCDs sequentially display red, green, and blue images to generate a full color image. Thus, FSC LCDs have advantages in high optical throughput, low material cost, high color saturation, and possibly three times higher resolution. However, CBU phenomenon and the critical LC response time limited the success of FSC method.

In order to solve these issues, we proposed the Stencil-LPD method without color filter. The Stencil-LPD method was proposed to further enhance the image quality in the field rate of 120Hz, so many commercial LC modes for currently using, such as MVA, TN, or IPS could be employed. The results presented that the color difference, using both average if CIEDE2000 and PDR($\Delta E_{00} > 3$) values as indices, of the reproduced image was acceptable for human eyes. Furthermore, the CBU visibility was also improved compared to the 2-color-field method. Therefore, the Stencil-LPD method is promising for low power consumption display using, especially for PIDs.

5.2 Future Works

Though the image quality was enhanced by using the Stencil-LPD method, some distortion would still show up when the image content is too complex. Thus, to lower the visibility of color difference due to this reason, a higher level feature analysis is needed. When there is too much color content in one segment, increasing the number of backlight

segment is not the only way to solve the two-field problem. The other way is to analyze the image content to choose the most two sensitive colors in the segment to human eye, such as the color of a patch instead of fragments. Here digital image processing is applied to analyze the image. In this way, the obvious color distortion can be reduced with less backlight segments. However, with higher level feature analysis, the complexity of computation is another issue to practical application. The more complicated computation process causes higher cost and more difficulty on hardware.

Besides, there is still not a criterion to judge color difference and CBU perceived by human eyes. The CIEDE2000 and $\Delta u'v'$ are often used to evaluate the image quality nowadays. However, different image complexity matters in the perceivable value of the indices. The acceptable value would be larger in the more complex image and vice versa. So here a criterion for the index is needed to judge how serious the color distortion in different image content is. Thus, human factor plays an important role here to help us defining the “just noticeable” value of the evaluation indices.



References

- [1] H. Hasabe and S. Kobayashi., "A Full-Color Field-Sequential LCD Using Modulated Backlight," *SID Symposium Digest Tech Papers*, p.81, 1985.
- [2] T. Miyashita, et. al., "Wide viewing-angle display mode for active-matrix LCDs using a bend-alignment liquid-crystal cell," *J. Soc. Info. Display*, vol. **3**(1), pp. 29-34, 1995.
- [3] F. Yamada, et. al, "Sequential-color LCD based on OCB with an LED backlight," *J. Soc. Info. Display*, vol. **10**, pp. 81-85, 2002.
- [4] J. H. Lee, et. al., "Novel color-sequential transfective liquid crystal displays," *J. Display Technol.*, vol. **3**(1), pp. 2-8, 2007.
- [5] M. G. Clark and I. A. Shanks, "A field-sequential color CRT using a liquid crystal color switching," in *Proceedings of SID Symposium Digest*, vol. **13**, pp. 172-173, 1982.
- [6] R. Vatne, et. al., "A LC/CRT field-sequential color display," in *Proceeding of SID Symposium Digest*, vol. **14**, pp. 28-29, 1983.
- [7] A. Yohso and K. Ukai, "How color break-up occurs in the human-visual system: The mechanism of the color break-up phenomenon," *J. Soc. Info. Display*, vol. **14**(12), pp. 1127-1133, 2006.
- [8] T. Ishinabe, et. al., "High performance OCB-mode for field sequential color LCDs," *SID Symposium Digest Tech Papers*, vol. **38**, pp 987-990, 2007.
- [9] T. W. Su, et. al., "Moving image simulation for high quality LCD TVs," *J. Soc. Info. Display*, vol. **15**(1), pp. 71-78, 2007.
- [10] K. Sekiya, et. al., "Spatio-temporal scanning LED backlight for large size field sequential color LCD," *IDW'05*, pp1261-1264, 2005.
- [11] Y. K. Cheng, et al., "Two- field scheme: Spatiotemporal modulation for Field Sequential Color LCDs," *J. Display Technol.*, vol. **5** (10), pp385-390, 2009
- [12] Y. Zhang, et al., "A hybrid spatial-temporal color display with Local-Primary-Desaturation backlight scheme," *J. Display Technol.*, vol. **7** (12), pp.665-673, 2011.
- [13] E. Langendijk, et al., "A novel spectrum-sequential display design with a wide color gamut and reduced color breakup," *J. Soc. Info. Display*, vol. **15** (4), pp. 261-266, 2007.

- [14] The Human Eye, retrieved on April 11, 2012, from the:
<http://users.rcn.com/jkimball.ma.ultranet/BiologyPages/V/Vision.html>
- [15] How We See: The First Steps of Human Vision, retrieved on April 11, 2012, from the:
http://www.accessexcellence.org/AE/AEC/CC/vision_background.php
- [16] Maxim Razin, after Bowmaker J.K., and Dartnall H.J.A., "Visual pigments of rods and cones in a human retina." *J. Physiol.* Vol. **298**, pp. 501-511, 1980.
- [17] J. Lee, et. al., "Noble measurement method for color breakup artifact in FPDs" in *IMID / IDMC Digest*, pp. 92-97, 2006.
- [18] Jiun-Haw Lee, et. al., *Introduction to Flat Panel Displays (1st ed)*, John Wiley & Sons, Ltd, 2008.
- [19] CIE 1931 color space, in Wikipedia, retrieved on June 20, 2012, from the:
http://en.wikipedia.org/wiki/CIE_1931_color_space
- [20] Mark D. Fairchild, *Color Appearance Models*. John Wiley & Sons, Ltd, 2005.
- [21] Roy S. Berns, *Principle of Color Technology*, John Wiley & Sons, Inc. pp. 63-121, 2000.
- [22] Good Jr, R.H. and Muller, E.W. Field emission, in *Handbook Der Physik, Vol. XXI, Electron-Emission Gas Discharge 1*, Springer-Verlag, Berlin, p. 176, 1956.
- [23] CIE, "Improvement to industrial colour-difference evaluation," *CIE Publication*, No. 142-2001, Central Bureau of the CIE, Vienna, 2001.
- [24] G. M. Johnson and M.D. Fairchild, "A top down description of S-CIELAB and CIEDE2000," *Color Research and Application*, vol. **28**, pp. 425-435, 2003.
- [25] M. R. Luo, G. Cui, and B. Rigg, "The development of the CIE 2000 colour difference formula," *Color Research and Application*, vol. **26**, pp. 340-350, 2001.
- [26] G. Sharma, W. Wu, and E. N. Dalal, "The CIEDE2000 Color-difference Formula: Implementation Notes, Supplementary Test Data and Mathematical Observations," *Color Research and Application*, vol. **30**, pp. 21-30, 2005.
- [27] K. Sekiya, T. Miyashita, and T. Uchida, "A Simple and Practical Way to Cope With Color breakup on Field Sequential Color LCDS," *SID Symposium Digest Tech Papers*, pp.1661-1664, 2006.
- [28] H. Yamakita, et. al., "Field-Sequential Color LCD driven by Optimized Method for Color Breakup Reduction," *International Display Workshop*, pp. 83-86, 2005.

- [29] F. C. Lin, et. al., "Color Breakup Suppression and Low Power Consumption by Stencil-FSC Method in Field-Sequential LCDs," *J. Soc. Info. Display*, vol. **17**(3), pp. 221-228, 2009.
- [30] F. C. Lin, et. al., "Color filter-less LCDs in achieving High Contrast and low power consumption by Stencil Field- Sequential-Color method," *J. Display Technol.*, vol. **6**(3), pp. 98-106, 2010.
- [31] F. C. Lin, et. al., "Color breakup reduction by 180 Hz Stencil-FSC method in large-sized color filter-less LCDs," *J. Display Technol.*, vol. **6**(3), pp. 107-112, 2010.
- [32] F. C. Lin, et al., "Color breakup suppression by Local primary Desaturation in Field-Sequential Color LCDs," *J. Display Technol.*, vol. **7** (2), pp.55-61, 2011.
- [33] Y. Zhang, et al., "A field-sequential-color display with a local-primary-desaturation backlight scheme," *Journal of SID*, vol. **19** (3), pp. 242-248, 2011.

